Crystal structure determination of *Escherichia coli* polyamine binding protein and molecular mechanism of polyamine binding

大腸菌ポリアミン結合蛋白質の結晶構造解析
とポリアミン結合の分子機構

Shigeru Sugiyama

Osaka University

1997

CONTENTS

Chapter 1 General Introduction 1

1.1 Polyamines and Anti-Cancer Drugs 2
1.2 Cell Membranes 3
1.3 Active Transport Systems 4
1.4 Substrate Binding Proteins 6
1.5 Polyamine Binding Proteins 7
References 9

Chapter 2 Crystallization and Preliminary X-ray Analysis of the Primary Receptor (PotD) of the Polyamine Transport System in *Escherichia coli.* 11

2.1 Abstract 12
2.2 Introduction 13
2.3 Crystallization and X-ray Diffraction 14
References 21

Chapter 3 Crystal Structure of PotD, the Primary Receptor of the Polyamine Transport System in *Escherichia coli.* 23

3.1 Abstract 24
3.2 Introduction 25
3.3 Materials and methods 26
3.3.1 Structure Determination
3.3.2 Model Building and Crystallographic Refinement
3.4 Results 30
3.4.1 Overall Structure of PotD
3.4.2 Subunit Contacts
3.4.3 Spermidine Binding
3.5 Discussion 39
3.5.1 Comparison with Other Periplasmic Binding Proteins
3.5.2 Open and Closed Forms
3.5.3 Dimer Formation
3.5.4 Spermidine Recognition
3.5.5 Consensus Motif
3.5.6 Interactions with the Membrane Bound Components
References 45

Chapter 4 Spermidine-preferential Uptake System in *Escherichia coli* Identification of Amino Acids Involved in Polyamine Binding in PotD Protein 49

4.1 Abstract 50
4.2 Introduction 51
4.3 Materials and methods 52
4.3.1 Bacterial Strains, Plasmids, and Culture Conditions
4.3.2 Mutagenesis of potD Gene
4.3.3 Polyamine Uptake by Right-side-out Membrane Vesicles
4.3.4 Assay for Polyamine Binding to PotD Protein
4.3.5 Spermidine Uptake by Intact Cells
4.4 Results 55
4.4.1 Spermidine and Putrescine Uptake Activities by Right-side-out Membrane Vesicles and Mutated PotD Protein
4.4.2 Spermidine and Putrescine Binding to Mutated PotD Protein
4.4.3 Spermidine Uptake Activities of Intact Cells Containing Mutated PotD Proteins
4.5 Discussion 62
References 66

Chapter 5 The 1.8 Å X-ray Structure of the *Escherichia coli* PotD Protein complexed with Spermidine and the mechanism of polyamine binding 69

5.1 Abstract 70
5.2 Introduction 71
5.3 Materials and methods 72
5.3.1 Crystal Structure Determination and Refinement
5.3.2 Modeling of the PotF Structure
5.4 Results and Discussion 75
5.4.1 Crystal Structure of the PotD-Spermidine Complex
5.4.2 Spermidine Binding
5.4.3 Substrate Specificity of Polyamine-Binding Proteins
References 90

Chapter 6 Concluding Remarks 93

List of Publications 99
Acknowledgements 101

Chapter 1

General Introduction

1.1 Polyamines and Anti-Cancer Drugs

Polyamines are low molecular weight compounds which are present in all organisms, both procaryotic and eucaryotic (1). The most widely distributed polyamines are putrescine, spermidine and spermine (Figure 1.1). They are involved in a variety of biological reactions, including nucleic acid and protein synthesis, and are essential components for cell proliferation.

The cellular polyamine contents are controlled by its metabolism in cell, and transport. The decrease of the cellular polyamine contents can inhibit cell proliferation. This means that a novel anti-cancer drug may be developed by controlling the following systems: the catabolism or uptake inhibitor, and the anabolism or excretion accelerator. The development of the polyamine catabolic inhibitors have been proceeded, because the earliest system revealed is the biosynthetic system of the polyamines. The inhibitors however, though they have a anti-cancer effect, do not come into practical use yet.

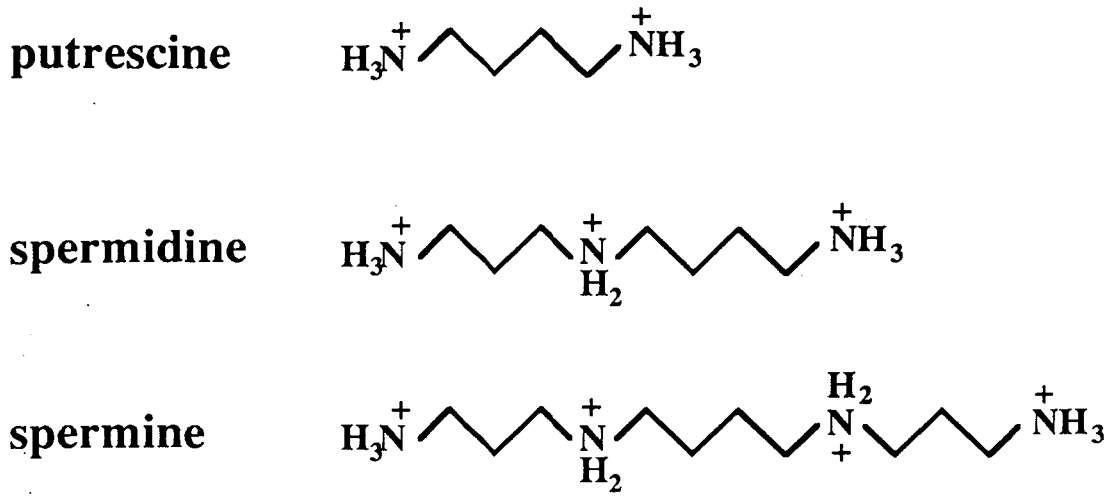

Figure 1.1 Polyamines

1.2 Cell Membranes

Cells are vitally dependent on transport processes, which maintain a relative constancy of the environment within cells and regulate the entrance or exit of various substances essential for metabolic activity. Many distinct transport systems for various substrates are at work within a certain cell type. In general, the systems in enteric bacteria have been more extensively characterized in terms of their biochemical processes (9).

The lipid bilayer of cell membranes serves as a barrier to the passage of most polar molecules, because of its hydrophobic interior. This barrier function is crucially important as it allows the cell to maintain the concentrations of solutes in its cytosol that are different from those in the extracellular fluid and in each of the intracellular membrane bounded compartments. To make use of this barrier, however, cells have had to evolve many devices of transferring specific water soluble molecules across their membranes in order to ingest essential nutrients, excrete metabolic waste products, and regulate intracellular ion concentrations. The transportation of inorganic ions and small water-soluble organic molecules across the lipid

bilayer is achieved by specialized transmembrane proteins, each of which is responsible for the transfer of the specific ion or molecule. The importance of membrane transport is indicated by the fact that almost 20 % of the genes identified so far in *E. coli* are associated with such transport processes.

1.3 Active Transport Systems

Some of the polyamine transport genes in *Escherichia coli* have been cloned and characterized by Igarashi *et al* (3). The proteins encoded by pPT104 and pPT79 operons constitute the spermidine preferential and the putrescine specific uptake system, respectively. These two systems are periplasmic transport systems which belong to the ABC transporter superfamily (4), for example, multidrug resistance (MDR) ATPase, chloroquine-resistance ATPase, mating pheromone exporter, and peptide pump in ER membrane (5). Each polyamine transport system consists of four proteins (6,7): pPT104 encodes the PotA, -B, -C, and -D proteins, and pPT79 encodes the PotF, -G, -H, and -I proteins (Figure 1.2). PotA and PotG proteins are bound to the inner surface of the cytoplasmic membrane. PotB, -C, -H, and -I proteins are transmembrane components that probably form polyamine transport channels. PotD and PotF proteins are periplasmic components. PotD protein binds both spermidine and putrescine, although spermidine is preferred (6). In contrast, PotF protein binds only putrescine (8).

The compounds which inhibit these transport systems, are candidates for anti-cancer drugs. By understanding the specificities of these transport systems based on three-dimensional structure, we will gain important information for the developement of novel anti-cancer drugs, since the inhibition of these transport systems may affect the cell proliferation.

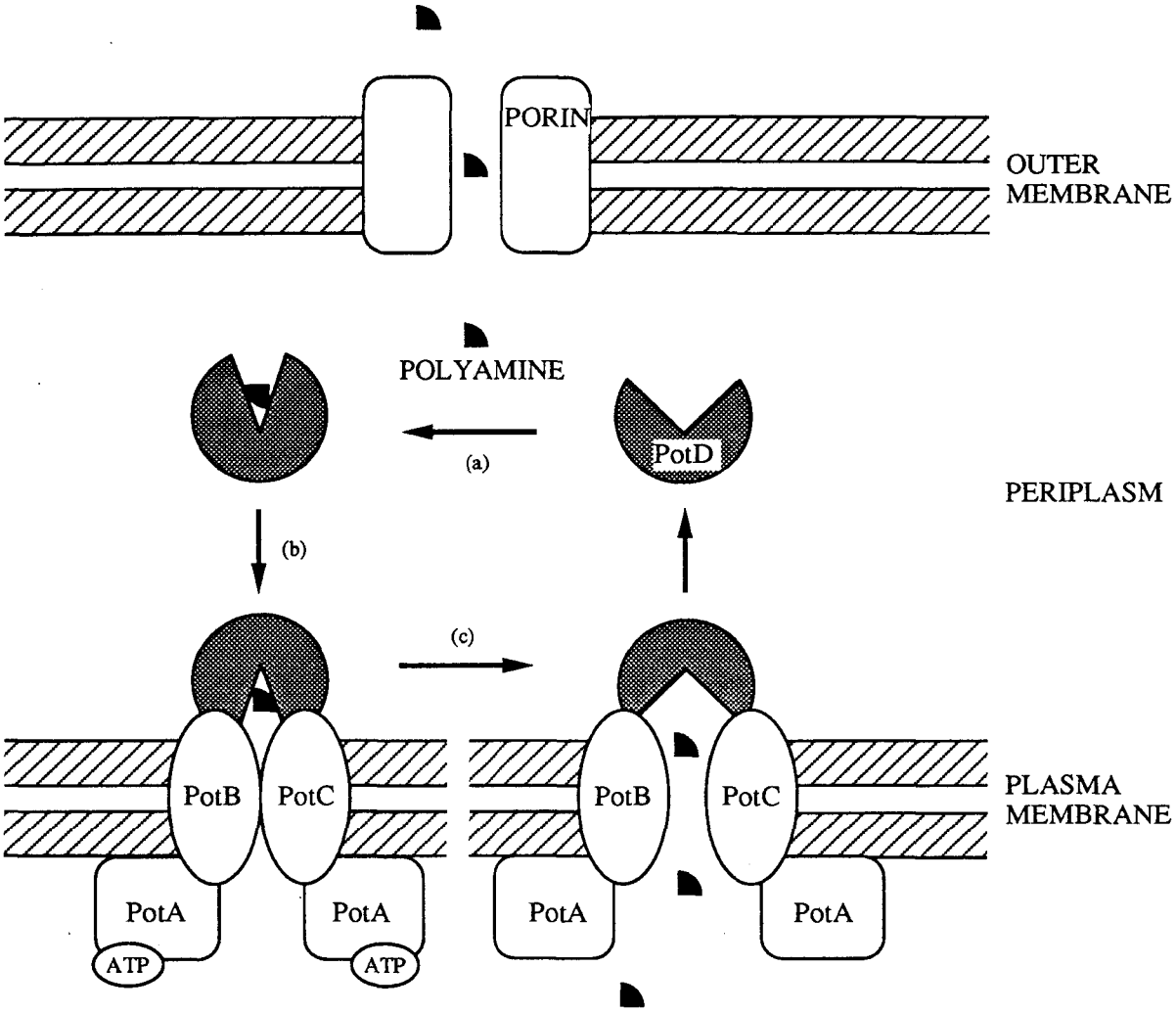

Figure 1.2 A model of polyamine transport system.

The polyamine diffuses through channel-forming proteins (called porin) in the outer membrane and binds to the PotD protein (a). As a result, the PotD protein undergoes a conformational change that enables it to bind to the PotB and/or PotC proteins (b), which then picks up the molecule and actively transfers it across the bilayer in a reaction driven by ATP hydrolysis of the PotA protein (c).

1.4 Substrate Binding Proteins

By harnessing different sets of protein components, the active transport systems carry out the uptake of different substrates. The periplasmic receptors or binding proteins serve as initial receptors for ligand recognition and tight binding. Furthermore, there are several of the binding proteins as primary receptor for bacterial chemotaxis. These binding proteins are present in the periplasmic space, a region between the outer wall and the cytoplasmic membrane. They consist of a single polypeptide chain with one high affinity ligand-binding site. The molecular masses of these proteins are in the range 23.0 - 55.0 kDa, with most around 33.0 kDa (10). The primary ligands are bound to these binding proteins with similar affinities (11). It is noteworthly that the Kd values of the receptor ligand complexes obtained from the kinetics and equilibrium measurements are similar to the *in vivo* Km values for transport (12). These ligand binding parameters are believed to be essential for the function receptors in both active transport and chemotaxis (11-16).

The crystal structures of several substrate-specific binding proteins in periplasmic space, such as amino acids (lysine/arginine/ornithine (17-19), leucine/isoleucine/valine (20), and leucine (21), histidine (22,23), glutamine (24)), oligopeptide (25), tetrahedral oxyanions (sulfate (26), and phosphate (27)), and saccharides (arabinose (28), galactose/glucose (29), ribose (30), and maltodextrin (31,32)) binding proteins have been solved by X-ray analyse. These proteins, which have remarkably broad specificities, share a similar main chain fold, although they lack significant sequence similarities. Furthermore, they consist of two similar domains, which show an "opening-closing" movement likened to a Venus flytrap, in depending upon substrate binding (32).

1.5 Polyamine Binding Protein

The polyamine binding proteins which firstly recognize the polyamines in the transport systems, are important target for the developement of anti-cancer drugs. The PotD protein which consists of 348 amino acids residues without a cystein residue, serves as an initial high affinity receptor. Its amino acid sequence have been compared with a library of 131 known structures including the other periplasmic binding proteins. It has been shown that the PotD protein is a structural similarity to maltodextrin-binding protein (MBP). The sequence alignment between PotD protein and MBP has revealed a conserved sequence motif (Figure 1.3). This motif exists also in an sequence of iron binding protein (IBP), which is an initial receptor of the periplasmic transport system. The highly conserved sequence motif observed in MBP, PotD, and IBP may suggest a common functional role in the transport system.

This thesis consists of six chapters. I deal with crystallization and preliminary X-ray analysis of the PotD protein in Chapter-2, and describe and discusse the polyamine binding activities and the structural features, resulted from three-dimensional structure of PotD protein in Chapter-3. Chapter-4 contains the identification of amino acids involved in polyamine binding by mutant PotD proteins, based on X-ray analysis as previously described in Chapter-3. The substrate specificity of polyamine binding proteins is discussed in Chapter-5, based on the results of the high resolution X-ray structure of PotD protein and the structure model of PotF protein.

Maltodextrin-binding protein (MBP)
Spermidine/putrescine-binding protein (PotD)

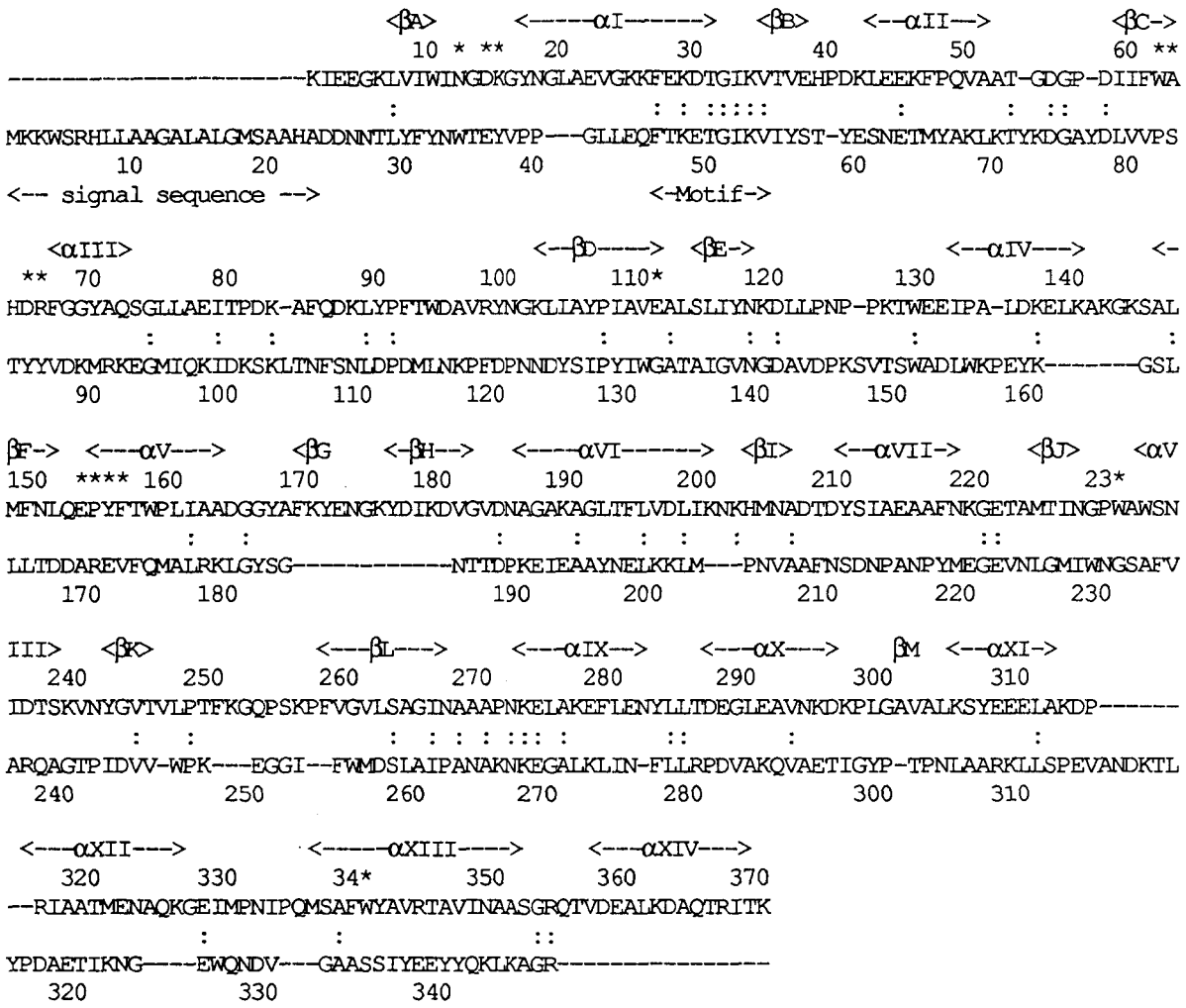

Figure 1.3

Alignment of the PotD protein sequence with the MBP structure.

The lines in the sequence denotes a gap inserted for the optimal alignment. Secondary structures (-helices and -strands) were defined for MBP using the DSSP program (31). Residues of MBP which are involved in ligand binding are indicated by the asterisks. A conserved sequence motif between PotD and MBP is indicated by <-*Motif*->.

References

1. Tabor, C. W., and Tabor, H. (1984) *Annu. Rev. Biochem.* **53**, 749-790
2. Pegg, A. E. (1988) *Cancer Res.* **48**, 759-774
3. Kashiwagi, K., Hosokawa, N., Furuchi, T., Kobayashi, H., Sasakawa, C., Yoshikawa, M., and Igarashi, K. (1990) *J. Biol. Chem.* **265**, 20893-20897
4. Ames, G. F. L. (1986) *Annu. Rev. Biochem.* **55**, 397-426
5. Higgins, C. F. (1995) *Cell* **82**, 693-696
6. Furuchi, T., Kashiwagi, K., Kobayashi, H., and Igarashi, K. (1991) *J. Biol. Chem.* **266**, 20928-20933
7. Pistocchi, R., Kashiwagi, K., Miyamoto, S., Nukui, E., Sadakata, Y., Kobayashi, H., and Igarashi, K. (1993) *J. Biol. Chem.* **268**, 146-152
8. Kashiwagi, K., Suzuki, T., Suzuki, F., Furuchi, T., Kobayashi, H., and Igarashi, K. (1991) *J. Biol. Chem.* **266**, 20922-20927
9. Lengeler, J. W., Titgemeyer, F., Vogler, A. P., and Wohrl, B. M. (1990) *Phil. Trans. R. Soc. Lond.* **326**, 489-504
10. Furlong, C. E. (1987) in Escherichia coli and Salmonella tryphimurium: Cellular and Molecular Biology (Neidhardt, F. C., Ingraham, J. L., Low, K. B., Magasanik, B., Schaechter, M., and Umbarger, H. E., eds) pp. 768-796, American Society for Microbiology, Washington, D. C.
11. Miller, D. M. III, Olson, J. S., Pflugrath, J. W., and Quiocho, F. A. (1983) *J. Biol. Chem.* **258**, 13665-13681
12. Miller, D. M. III, Olson, J. S., and Quiocho, F. A. (1980) *J. Biol. Chem.* **255**, 2465-2471
13. Quiocho, F. A. (1984) *Proc. R. A. Welch. Found. Conf. Chem. Res.* **27**, 333-358
14. Quiocho, F. A., and Vyas, N. K. (1984) *Nature* **310**, 381-386
15. Pflugrath, J. W., and Quiocho, F. A. (1988) *J. Mol. Biol.* **200**, 163-180

16. Quiocho, F. A. (1990) *Phil. Trans. R. Soc. Lond.* **326**, 341-351
17. Kang, C. H., Shin, W. C., Yamagata, Y., Gokcen, S., Ames, G. F. L., and Kim, S. H. (1991) *J. Biol. Chem.* **266**, 23893-23899
18. Oh, B. H., Pandit, J., Kang, C. H., Nikaido, K., Gokcen, S., Ames, G. F. L., and Kim, S. H. (1993) *J. Mol. Biol.* **268**, 11348-11355
19. Oh, B. H., Ames, G. F. L., and Kim, S. H. (1994) *J. Biol. Chem.* **266**, 26323-26330
20. Sack, J. S., Saper, M. A., and Quiocho, F. A. (1989) *J. Mol. Biol.* **206**, 171-191
21. Sack, J. S., Trakhanov, S. D., Tsigannik, I. H., and Quiocho, F. A. (1989) *J. Mol. Biol.* **206**, 193-207
22. Oh, B. H., Kang, C. H., Bondt, H. D., Kim, S. H., Nikaido, K., Joshi, A. K., and Ames, G. F. L. (1994) *J. Biol. Chem.* **269**, 4135-4143
23. Yao, N., Trakhanov, S., and Quiocho, F. A. (1994) *Biochemistry* **33**, 4769-4779
24. Hsiao, C. D., Sun, Y. J., Rose, J., and Wang, B. C. (1996) *J. Mol. Biol.* **262**, 225-242
25. Tame, J. R. H., Murshudov, G. N., Dodson, E. J., Neil, T. K., Dodson, G. G., Higgins, C. F., and Wilkinson, J. A. (1994) *Science* **264**, 1578-1581
26. Pflugrath, J. W., and Quiocho, F. A. (1988) *J. Mol. Biol.* **200**, 163-180
27. Luecke, H., and Quiocho, F. A. (1990) *Nature* **347**, 402-406
28. Quiocho, F. A., and Vyas, N. K. (1984) *Nature* **310**, 381-386
29. Vyas, N. K., Vyas, M. N., and Quiocho, F. A. (1988) *Science* **242**, 1290-1295
30. Mowbray, S. L., and Cole, L. B. (1992) *J. Mol. Biol.* **225**, 155-175
31. Sharff, A. J., Rodseth, L. E., Spurlino, J. C., and Quiocho, F. A. (1992) *Biochemistry* **31**, 10657-10663
32. Spurlino, J. C., Lu, G. Y., and Quiocho, F. A. (1991) *J. Biol. Chem.* **266**, 5202-5219

Chapter 2

Crystallization and preliminary X-ray analysis of the primary receptor (PotD) of the polyamine transport system in *Escherichia coli*

2.1 Abstract

The primary receptor (PotD, M_r 39000) of the polyamine transport system in *Escherichia coli* was crystallized by the vapor-diffusion method. Two crystal forms were obtained in the presence of spermidine, and were examined by X-ray analysis. Form I crystals, which diffract to 2.5 Å resolution, belong to the space group $P\,2_1$, with unit cell dimensions a = 145.3, b = 69.1, c = 72.5 Å and β = 107.6°. Four molecules are contained in an asymmetric unit. These form two dimers that are related to each other by a local translation of about half of the unit cell along the a axis. The two protein molecules in each dimer are similarly related by a local dyad. Form II crystals diffract to 1.8 Å resolution and belong to the space group $I\,4_1$, with unit cell dimensions a = b = 130.3 and c = 38.7 Å. They contain one molecule per asymmetric unit.

2.2 Introduction

Polyamines, such as putrescine, spermidine, and spermine, are ubiquitous in all living organisms, and are implicated in a wide variety of biological reactions, including nucleic acid and protein syntheses (1,2). It is a crucial subject in cell biology to understand the detailed mechanisms of polyamine biosynthesis and transport, by which the cellular polyamine contents are controlled. Although the biosynthetic pathways for polyamines have been studied extensively, the transport mechanism remains obscure (1,2). The polyamine transport gene (pPT104) in *Escherichia coli* has been cloned and characterized (3). The proteins encoded by pPT104 constitute the spermidine preferential uptake system, which belongs to a periplasmic transport system (4,5). This spermidine transport machinery consists of four protein subunits, PotA, -B, -C, and -D, the primary structures of which have been deduced from the nucleotide sequences of the clones (6,7). The PotA (M_r 43000) protein, which is associated with the inner surface of the cytoplasmic membrane, is a strong candidate for an ATP hydrolyzing energy generating factor. In fact, the PotA protein contains a consensus nucleotide binding sequence, which is similar to the sequences of the α and β subunits of *E. coli* ATPase (8), the HisP protein (9), and the MalK protein (10). Both the PotB (M_r 31000) and PotC (M_r 29000) proteins have six transmembrane spanning segments linked by hydrophilic segments of variable length, and they probably form channels for spermidine and putrescine. The PotD protein is a polyamine binding protein present in the periplasmic space, and it regulates the polyamine content in cells. This protein binds both putrescine and spermidine, although it preferentially binds spermidine (11). To obtain more detailed insight into the molecular mechanism of the preferential spermidine transport, we have initiated a crystallographic study of the PotD protein.

2.3 Crystallization and X-ray Diffraction

The PotD protein was purified according to the protocol described previously (6). The purity was verified by sodium dodecyl sulfate polyacrylamide electrophoresis (SDS-PAGE). For crystallization, the protein was concentrated using a Centriprep-10 concentrator. In the presence of spermidine, crystals appeared in two different forms, which were designated as forms I and II (Figure 2.1). Form I was most frequently grown at 285 K by the sitting-drop mode of the vapor diffusion method. A protein solution containing 5 - 10 mg protein/ml, 10 mM Bis-tris buffer (pH 7.0), and 20 mM spermidine trihydrochloride was mixed with an equal volume of a reservoir solution containing 30% (w/v) polyethyleneglycol 10000 and 20 mM Bis-tris buffer (pH 7.0). The form I crystals were grown to an average size of 1.3 x 0.6 x 0.2 mm within three weeks. The form II crystals were produced by combining the techniques of vapor diffusion and repeated seeding. The crystallization solutions were prepared by mixing an equal volume of the protein solution and the reservoir solution. The protein solutions contained 5 - 10 mg protein/ml and 20 mM spermidine trihydrochloride in 10 mM HEPES buffer (pH 7.0), while the reservoir solution contained 30% (w/v) polyethyleneglycol 4000 and 40 mM HEPES buffer (pH 7.0). Small crystals appeared within a week. Repeated seeding was carried out to produce diffraction quality crystals. Before seeding, the mixture had been equilibrated at room temperature with adequate reservoir solutions for at least two days, and the seeds were introduced into the mixture within a week. Thus, suitable crystals for X-ray diffraction were obtained, with dimensions of 0.6 x 0.6 x 0.4 mm. Interestingly, small form II crystals sometimes appeared on the surface of the crystallization drops under the conditions that produce the form I, although these form II crystals did not grow large. No crystals could grow

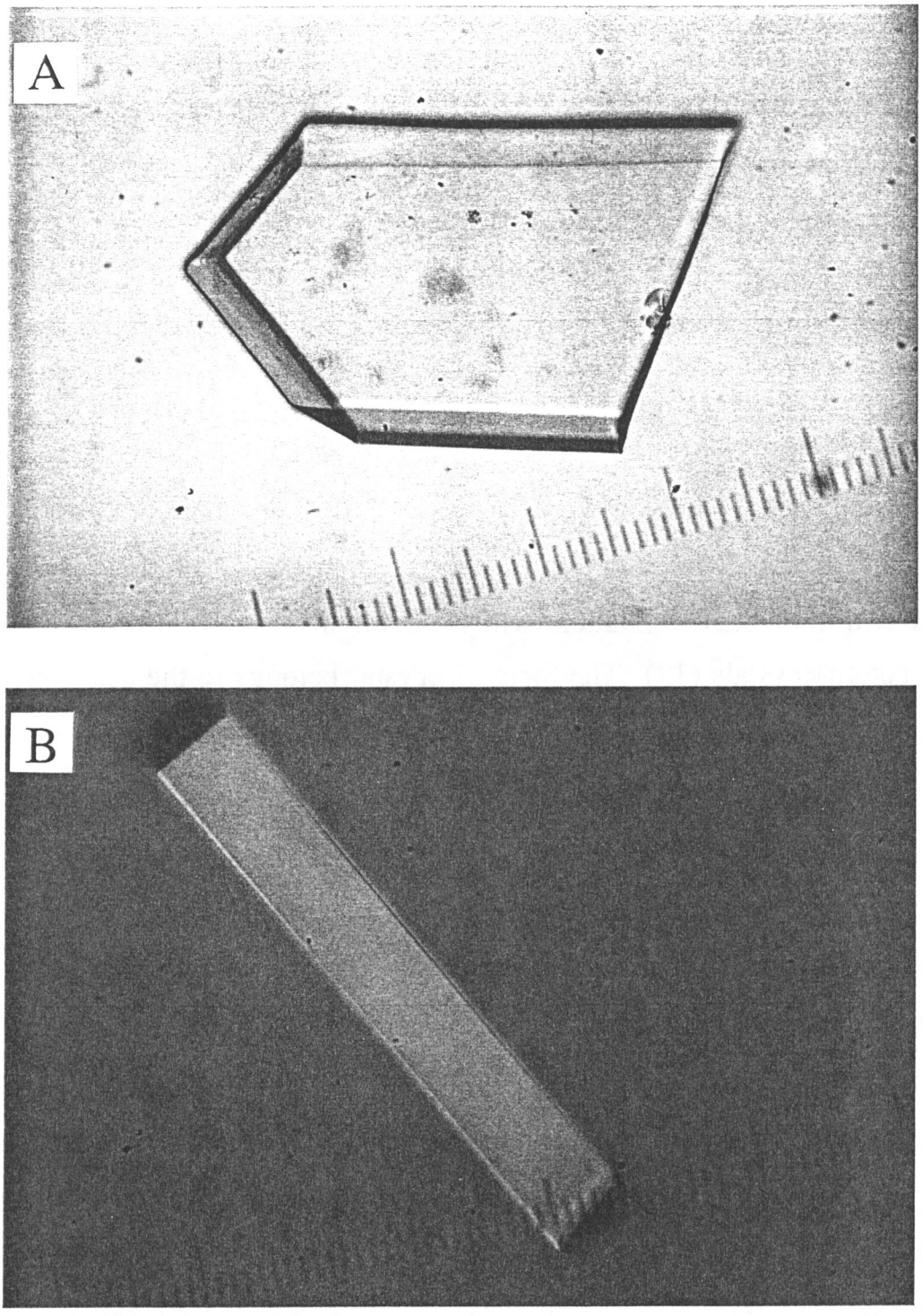

Figure 2.1

Crystals of PotD protein in complex wth spermidine.

A, Form I crystal. Maximum dimentions are 0.15 x 0.4 x 0.6 mm. The longest axis is parallel to the c-axis. B, Form II crystal. The crystals was grown by macro-seeding method step by step. Maximum dimentions are 0.2 x 0.2 x 1.0 mm. The longest axis is parallel to the c-axis.

in crystallization solutions lacking spermidine trihydrochloride. This result implies that the conformation of the PotD protein might be different, depending upon the presence or absence of the substrate.

Diffraction studies were carried out using a precession camera (Enraf Nonius & Huber). The diffraction patterns of the form I crystals exhibit systematic weakness of the $h = 2n + 1$ reflections at lower resolution. The form I crystal was found to belong to the space group $P\ 2_1$, with unit cell dimensions: a = 145.3, b = 69.1, c = 72.5 Å and β = 107.6°. There are four molecules in an asymmetric unit. The packing density of the crystal, Vm, is calculated to be 2.24 $Å^3$/Dalton, which is well within the range normally found for protein crystals (12). The form II crystal belongs to the space group $I\ 4_1$, with unit cell parameters: $a = b$ = 130.3 and c = 38.7 Å, and contains one molecule in an asymmetric unit. It has a similar solvent content to that of the form I crystal.

Intensity data were collected from each crystal form, using an automated oscillation camera system (DIP-320, MAC Science) with a cylindrical imaging plate detector (13,14), which is equipped on a Cu rotating anode generator operated at 50 kV, 90 mA at 277 K. The intensities recorded on the area detector were evaluated by the program WELMS (15), and were processed by the program PROTEIN (16). The completeness of their reflections of the crystal forms I and II for the intensity data ($I > 2\sigma(I)$) were 76.5 % to 2.7 Å resolution and 90.0 % for the data to 1.8 Å resolution, respectively. The Rmerge values were 5.3 % for the intensity data of crystal form I, and 5.6 % for those of crystal form II. Furthermore, another 2.5 Å resolution data set has been collected from the form I crystal, using the macromolecular-oriented Weissenberg camera (17), installed at the Beam Line 6A2 of the Synchrotron Radiation Source in the National Laboratory for High Energy Physics, Tsukuba. The wavelength was set to 1.00 Å. The diffraction patterns were digitized by a BA-100 reader (Fuji film). The intensity data were evaluated

using the program WEIS (18), and were processed by the programs COMBINE and SCALE from the same program package. These programs were implemented on a FACOM VP2600 vector computer. The completeness and the Rmerge value of this data set were 78.0 and 6.0 %, respectively. It should be noted that the diffraction pattern from the form I crystal systematically indicates weak intensities for the *h* odd indexed reflections (Figure 2.2). On the other hand, no remarkable intensity difference could be observed between the *h+k* even and odd indexed reflections. These findings suggest that half of the four independent protein molecules were related to the other half by local translation of about 1/2 of the unit cell length, along the *a* axis.

The self-rotation function was calculated for the resolution range from 10.0 to 3.5 Å, using the program X-PLOR (19). One significant peak, which is 1.33 times larger than the second highest peak, was observed on the section $\kappa = 180°$, indicating the presence of noncrystallographic 2-fold symmetry. The position of the peak yields the polar angles $\psi = 90°$, $\varphi = 36°$, and $\kappa = 180°$ (Figure 2.3). Thus, the noncrystallographic 2-fold axis is found to be approximately perpendicular to the crystallographic *b* axis. These results suggest that the protein molecules in the pair are related by the 2-fold axis, and that two pairs were packed with a local translation of about 1/2 of the unit cell length, along the *a* axis. The observation of a strong non-origin peak at approximately (0.5, 0, 0) in the Patterson synthesis is consistent with the above interpretation (Figure 2.4).

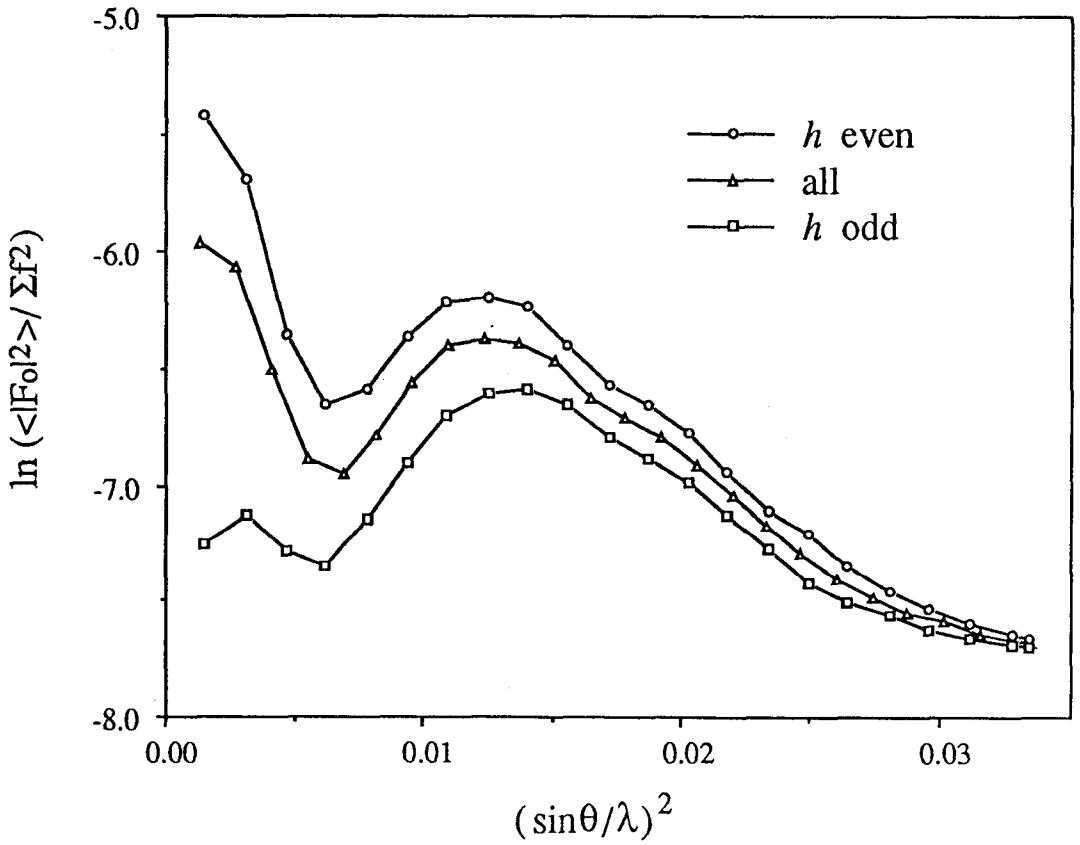

Figure 2.2

Wilson plot for the form I crystal with the intensity data to 2.7 Å resolution.

The intensity data are classified into three groups, in which the indexes of the reflections are $h = 2n$ and $h = 2n+1$. The $\langle|F_o|^2\rangle$ values of the h odd reflections are notably weaker than those of the h even indexed reflections, and in particular, at low resolution. This fact implies that similarly oriented protein molecules were packed in the unit cell with a local translation of about 1/2 of the unit cell length, along the a axis.

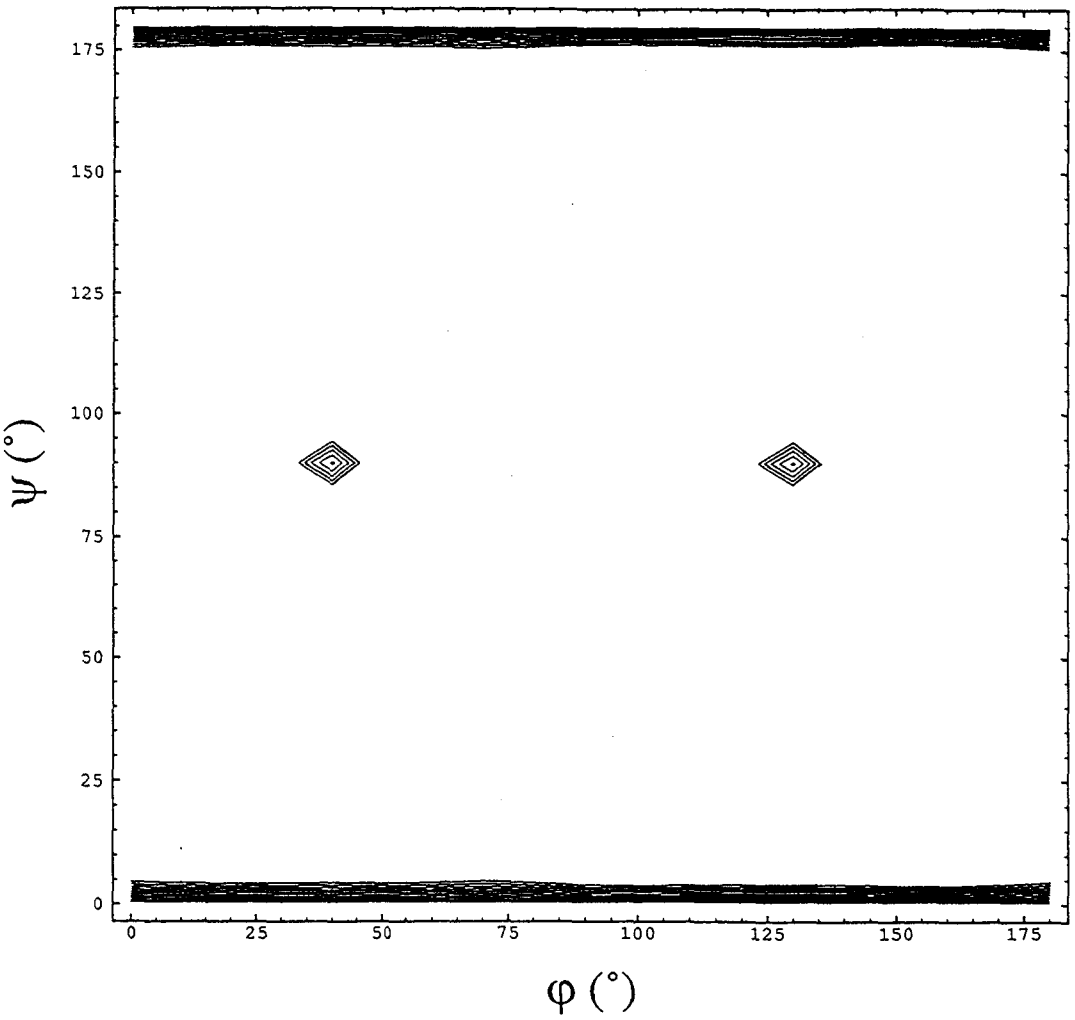

Figure 2.3

The κ = 180° plane of the self-rotation function for the form I crystal.

A total of 16,043 reflections between 10.0 and 3.5 Å resolution were included in the calculations. A single peak and its symmetry equivalent peak were found at polar angles $\psi = 90°$, $\varphi = 36°$ and 126°, $\kappa = 180°$, respectively.

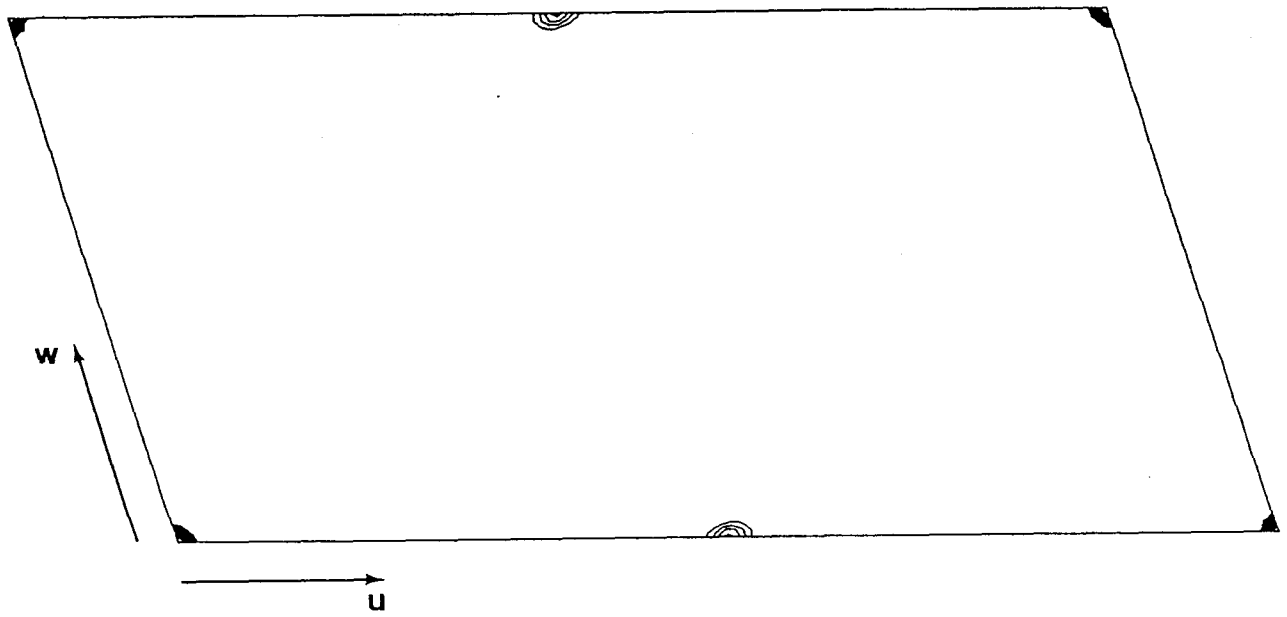

Figure 2.4

Patterson map of the form I crystal at the section, $v = 0$.

The map was calculated with all of the structure factors between 15.0 and 3.0 Å resolution. The origin peak is scaled to a value of 100, and the map has been contoured from 3 to 80 in steps of 6. The peak height at (0.5, 0, 0) is about 0.25 times that of the origin peak.

References

1. Tabor, C. W. & Tabor, H. (1984) *Annu. Rev. Biochem.* **53,** 749-790
2. Pegg, A. E. (1988) *Cancer Res.* **48**, 759-774
3. Kashiwagi, K., Hosokawa, N., Furuchi, T., Kobayashi, H., Sasakawa, C.,Yoshikawa, M. & Igarashi, K. (1990) *J. Biol. Chem.* **265**, 20893-20897
4. Ames, G. F. L. (1986) *Annu. Rev. Biochem.* **55**, 397-426
5. Furlong, C. E. (1987) In *Escherichia coli and Salmonella typhimurium: Cellular and Molecular Biology* , edited by Neidhardt, F. C., Ingraham, J.L., Low, K. B., Magasanik, B., Schaechter, M. & Umbarger, H. E., pp. 768-796. American Society for Microbiology, Washington, D.C.
6. Furuchi, T., Kashiwagi, K., Kobayashi, H. & Igarashi, K. (1991) *J. Biol. Chem.* **266**, 20928-20933
7. Pistocchi, R., Kashiwagi, K., Miyamoto, S., Nukui, E., Sadakata, Y., Kobayashi, H. & Igarashi, K. (1993) *J. Biol. Chem.* **268**, 146-152
8. Walker, J. E., Saraste, M., Runswick, M. J. & Gay, J. (1982) *EMBO J.* **1**, 945-951
9. Higgins, C.F., Haag, P.D., Nikaido, K., Ardeshir, F., Garcia, G. & Ames, G.F.-L. (1982) *Nature.* **298**, 723-727
10. Gilson, E., Nikaido, H. & Hofnung, M. (1982) *Nucleic Acids Res.* **10**, 7449-7458
11. Kashiwagi, K., Miyamoto, S., Nukui, E., Kobayashi, H. & Igarashi, K. (1993) *J. Biol. Chem.* **268**, 19358-19363
12. Matthews, B.W. (1968) *J. Mol. Biol.* **33**, 491-497
13. Miyahara, J., Takahashi, K., Amemiya, Y., Kamiya, N. & Satow, Y. (1986) *Nucl. Instrum. Methods A.* **246**, 572-578

14. Amemiya, Y., Matsushima, T., Nakagawa, A., Satow, Y., Miyahara, J. & Chikawa, J. (1988) *Nucl. Instrum. Methods A.* **266**, 645-653
15. Tanaka, I., Yao, M., Suzuki, M., Hikichi, K., Matsumoto, T., Kozasa, M. & Katayama, C. (1990) *J. Appl. Crystallogr.* **23**, 334-339
16. Steigemann, W. (1974) Ph. D. thesis, Technishe Universität, München.
17. Sakabe, N. (1991) *Nucl. Instrum. Methods Phys. Res.* **A303**, 448-463
18. Higashi, T. (1989) *J. Appl. Crystallogr.* **22**, 9-18
19. Brünger, A. T. (1990) *Acta Cryst.* **A46**, 46-57

Chapter 3

Crystal Structure of PotD, the Primary Receptor of the Polyamine Transport System in *Escherichia coli*

3.1 Abstract

PotD protein is a periplasmic binding protein and the primary receptor of the polyamine transport system, which regulates the polyamine content in *Escherichia coli*. The crystal structure of PotD in complex with spermidine has been solved at 2.5 Å resolution. The PotD protein consists of two domains with an alternating β–α–β topology. The polyamine binding site is in a central cleft lying in the interface between the domains. In the cleft, four acidic residues recognize the three positively charged nitrogen atoms of spermidine, while five aromatic side chains anchor the methylene backbone by van der Waals interactions. The overall fold of PotD is similar to that of other periplasmic binding proteins, and in particular, to the maltodextrin-binding protein from *E. coli*, despite the fact that sequence identity is as low as 20%. The comparison of the PotD structure with the two maltodextrin binding protein structures, determined in the presence and absence of the substrate, suggests that spermidine inding rearranges the relative orientation of the PotD domains to create a more compact structure.

3.2 Introduction

Polyamines, such as putrescine, spermidine, and spermine, are ubiquitous in all living organisms. They are involved in a wide variety of biological reactions, including nucleic acid and protein synthesis (1,2). These compounds exist as linear molecules with two (putrescine: NH_3^+-$(CH_2)_4$-NH_3^+), three (spermidine: NH_3^+-$(CH_2)_3$-NH_2^+-$(CH_2)_4$-NH_3^+), and four (spermine: NH_3^+-$(CH_2)_3$-NH_2^+-$(CH_2)_4$-NH_2^+-$(CH_2)_3$-NH_3^+) positively charged nitrogen atoms. It is a crucial subject in cell biology to elucidate the detailed mechanisms of polyamine biosynthesis and transport, by which the cellular polyamine contents are controlled. Although the biosynthetic pathways for polyamines have been studied extensively, the transport mechanism remains obscure (1,2).

The polyamine transport genes in *Escherichia coli* have been cloned and characterized (3-7). The proteins encoded by pPT104 constitute the spermidine preferential uptake system, which belongs to a periplasmic transport system (8,9). This spermidine transport machinery consists of four protein subunits, PotA, -B, -C, and -D. The PotA (M_r 43,000) protein, which is bound to the inner surface of the cytoplasmic membrane, is a strong candidate for an ATP-hydrolyzing, energy-generating factor. In fact, the PotA protein contains a consensus nucleotide binding sequence, and exhibits ATPase activity (10). Both the PotB (M_r 31,000) and PotC (M_r 29,000) proteins have six transmembrane spanning segments linked by hydrophilic peptides with variable lengths, and hence they are assumed to jointly form a channel for spermidine and putrescine. The PotD protein is a periplasmic binding protein and consists of 348 amino acids, corresponding to a molecular mass of 39kDa. Although it binds both spermidine and putrescine, spermidine is preferred (6).

The crystal structures of several periplasmic binding proteins specific for substrates, such as amino acids (lysine/arginine/ornithine (11,12), leucine/isoleucine/valine (13), and leucine (14)), oligopeptide (15), tetrahedral oxyanions (sulfate (16), and phosphate (17)), and saccharides (arabinose (18), galactose/glucose (19), ribose (20), and maltodextrin (21,22)) have been solved by X-ray analysis. These binding proteins, which have remarkably broad specificities, share a similar main chain fold, although they lack significant sequence similarities. Furthermore, they consist of two similar domains, which show an "opening-closing" movement likened to a Venus flytrap, depending upon substrate binding (22).

The polyamines are unique substrates for a periplasmic binding protein. Their specific interactions with cognate binding proteins have never been studied in terms of three-dimensional structure. Therefore, a crystallographic study of the PotD protein at an atomic resolution was performed to elucidate the detailed mechanism of its specific substrate recognition and the characteristics of the main chain folding. In this paper, we report the molecular structure of the PotD-spermidine complex determined at 2.5 Å resolution by X-ray analysis.

3.3 Materials and methods

3.3.1 *Structure Determination*

The form I crystals, which belong to the monoclinic system space group $P\,2_1$, with unit cell parameters a = 145.3 Å, b = 69.1 Å, c = 72.5 Å, and β = 107.6°, were grown according to the procedure described previously (24). They contain four molecules in the asymmetric unit. The procedure for data collection was already reported (24).

The major heavy atom sites of K_2PtCl_4 and $Pb(NO_3)_4$ derivatives prepared by soaking were determined from their difference Patterson maps. The initial analysis of the X-ray data showed that the structure factors for the reflections with the odd h indices were much smaller than those with the even h indices ($<F(2n+1,k,l)> = 0.5*<F(2n,k,l)>$) in a 6.0 Å resolution shell. This fact, along with the analysis of the heavy atom sites in the derivatives, confirmed that there are two dimers of the protein in the asymmetric unit, connected by an almost precise translational symmetry with 1/2 of the a axis of the crystal (24). The heavy atom parameters were refined with the programs PROTEIN (25) and MLPHARE (26) against the 3.0 Å resolution data, including anomalous data from all derivatives. The latter program provided the mean figure of merit of 0.63. Solvent flattening (27) and noncrystallographic symmetry averaging techniques (28) were applied to improve the phases. The 2-fold molecular averaging, using only reflections with $h=2n$, was successful in substantially improving the map. However, this map was still insufficient to achieve a complete chain tracing. The structure determination statistics for the MIR phasing are summarized in Table 3.1.

3.3.2 *Model Building and Crystallographic Refinement*

The initial model was constructed on the basis of the averaged electron density map at 3.0 Å resolution, using the program O (29). Rigid body refinement was then carried out using the program X-PLOR, version 3.0 (30) with all the data to 3.0 Å resolution. The initial model was used to define the molecular envelope, and then the 4-fold averaging technique was repeated using all the data, for further improvement of the phases, by the program DM in the CCP4 package (26). The averaging was reiterated until convergence was achieved, while the phases were expanded from 3.0 to 2.7 Å resolution. The correlation coefficients increased from 0.33 to 0.85. Consequently, this map allowed us to achieve a complete chain tracing. The model was manually

Table 3.1

Structure determination statistics of PotD

Data set[a]	Instrument[b]	Unique reflections		R_{merge}[c]	R_{iso}[d]	Phasing	R_{Cullis}[f]
		Number	Completeness	(all data)		power[e]	
			%	%	%		
Native	PF (2.5 Å)	38,903	81.6	6.79			
Native	DIP320 (2.7 Å)	28,546	75.1	5.71			
Combined	(2.5 Å)	40,242	84.4	9.45			
PTCL1	DIP320 (3.0 Å)	9698	69.9	8.86	21.3	1.89	0.57
PTCL2	DIP320 (3.0 Å)	9853	71.0	7.65	22.2	1.78	0.63
PBNO	DIP320 (3.0 Å)	10,284	74.1	7.68	13.0	1.36	0.70
UONO	DIP320 (3.0 Å)	9410	67.8	7.88	25.3	1.17	0.79
KUOF	DIP320 (3.0 Å)	8649	62.3	9.06	25.4	1.20	0.78

Resolution	10.00	7.50	6.00	5.00	4.29	3.75	3.33	3.00	Total
Figure of merit	0.68	0.72	0.71	0.70	0.68	0.63	0.59	0.53	0.63

[a] PTCL1, 5mM K_2PtCl_4; PTCL2, 1mM K_2PtCl_4; PBNO, 5mM $Pb(NO_3)_2$; UONO, 1mM $UO_2(NO_3)_2$; KUOF, 1mM $K_2UO_3F_5$.

[b] Resolution is shown in parentheses.

[c] $R_{merge} = \Sigma\Sigma|I_{hj} - \langle I_h \rangle|/\Sigma\Sigma\langle I_h \rangle$

[d] $R_{iso} = \Sigma||F_{PH}| - |F_P||/\Sigma|F_P|$

[e] Phasing power, the ratio of the root mean square (r.m.s.) heavy-atom scattering factor amplitude to the r.m.s. lack of closure error.

[f] $R_{Cullis} = \Sigma||F_{PH} \pm F_P| - F_{H(CALC)}|/\Sigma|F_{PH} - F_P|$ (for centric reflections), Where I_{hj} = measured diffraction intensity; $\langle I_h \rangle$ = mean value of all intensity measurements of (h,k,l) reflections, F_{PH} = structure amplitude of a derivative, F_P = structure amplitude of the native crystal, and $F_{H(CALC)}$ = the calculated contribution of the heavy atoms.

modified by the program FRODO (31) on an Evans & Sutherland PS390 graphics system, and it was refined against the 2.5 Å resolution data set, using the program X-PLOR. During the refinement, the ($|F_o| - |F_c|$) and ($2|F_o| - |F_c|$) maps were used for manual adjustments of the model, and for locating the four spermidine and the solvent molecules. Only the water molecules that form geometrically reasonable hydrogen bonds with the protein atoms were included in the refinement calculation. The Ramachandran plots for the main chain torsion angles have been analyzed with the PROCHECK program (32), and the ψ and φ torsion angles for the nonglycine residues lie within the allowed regions. The overall geometry of the model is satisfactory, as shown in Table 3.2.

Table 3.2
Refinement statistics

The *R*-factor for all data (36,198 reflections) with $F>1.0\sigma(F)$ between 6 and 2.5 Å resolution is 0.207. The free *R*-factor (45) was calculated from a random selection comprising 10% of all data with $F>1.0\sigma(F)$. The r.m.s. deviations are from the ideal values derived from Engh and Huber (46).

Number of protein atoms (non-hydrogen)	10,240
Number of ligand atoms	40
Number of water molecules	236
R-factor	0.199[F>1.0σ(F)]
R-free	0.280
r.m.s. deviation in bond lengths	0.016 Å
r.m.s. deviation in bond angles	1.98°
r.m.s. deviation in improper torsions	1.80°

3.4 Results

3.4.1 *Overall Structure of PotD*

The crystal contains two dimeric molecules of the PotD protein in the asymmetric unit. The final structure refined at 2.5 Å resolution includes four identical protein molecules, each of which contains 325 amino acids, and one ordered spermidine molecule, in addition to 236 ordered water molecules in the asymmetric unit. The first two residues (aspartate residues 24 and 25) at the N terminus (since the signal sequence is eliminated in the crystallized PotD protein, Asp24 is defined as the N terminal residue) are not well defined in the electron density map, and their conformations appear to be disordered in the crystal. The primary sequence with the secondary structure elements and the ribbon representation are shown in Figure 3.1.

The PotD molecule has an ellipsoidal shape with dimensions of 30 x 40 x 55 Å. It consists of two distinct domains divided by a deep cleft. Each domain is formed by two noncontiguous polypeptide segments. Nevertheless, the two domains are very similar in the arrangements of their secondary structure elements. The first domain (N domain: residues 26 - 131 and 257 - 302) consists of five β strands and six α helices. The other domain (C domain: residues 132 - 256 and 303 - 348), with a larger size, contains five β strands and seven α helices. The β sheet within each domain is flanked by several α helices on both sides. The polypeptide chain crosses over three times between the two domains, which noncovalently interact with each other by an extensive interface. The three crossing segments and the interface form a deep cleft with approximate dimensions of 20 Å long, 5 Å wide, and 14 Å deep (Figure 3.1B). The PotD protein, with its many β–α–β repeats, is classified as an α/β type. Of the amino acids, 40 and 18 % are located in the α helices and the β sheets, respectively. The remaining amino acids (42 %) belong to loops and coils.

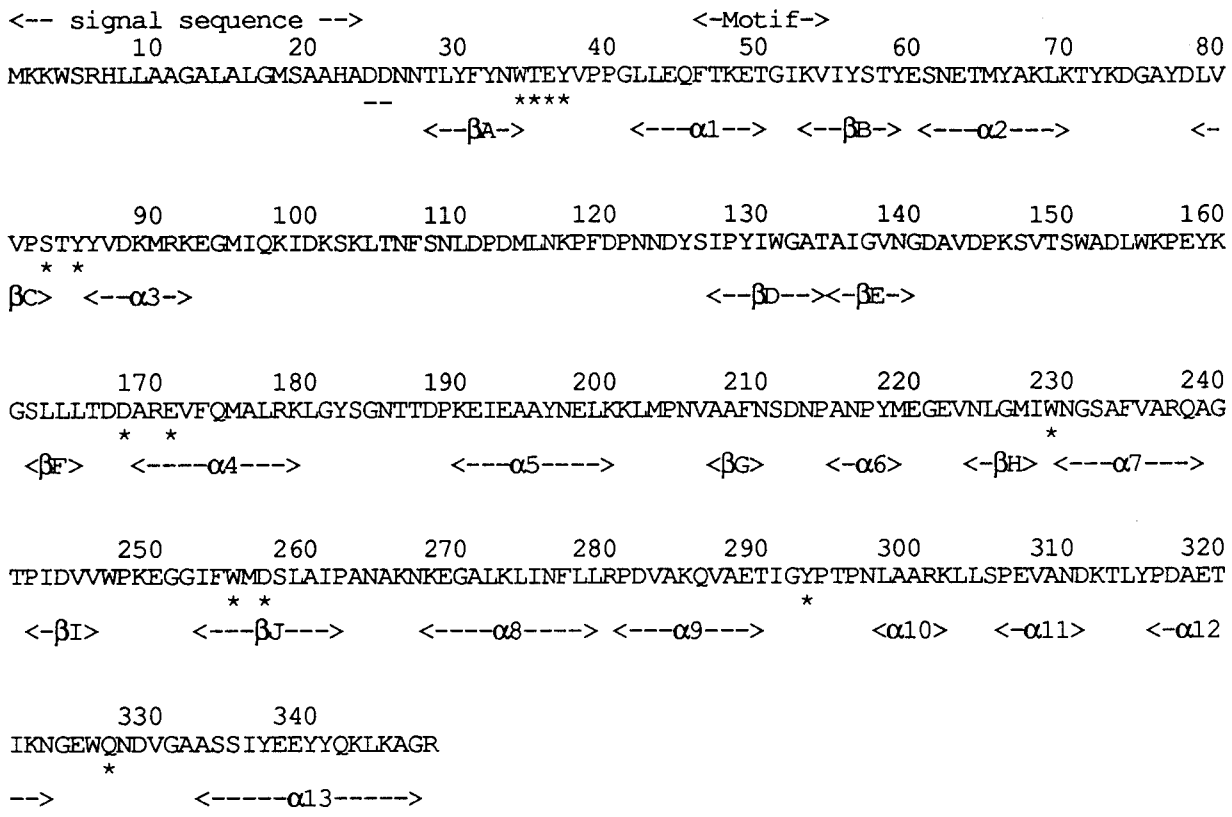

Figure 3.1(A) Structure of the PotD.

Primary sequence of the PotD protein with the secondary structure elements. The amino acid sequence has been deduced from the base sequence of the *pot*D gene (6). Residues involved in ligand binding are indicated by an *asterisk*. The underlines indicate a disordered region (Asp^{24} and Asp^{25}) in the crystal. A conserved sequence motif between PotD and MBP is indicated by <-*Motif*->, and spans residues 46 - 54 of PotD (35).

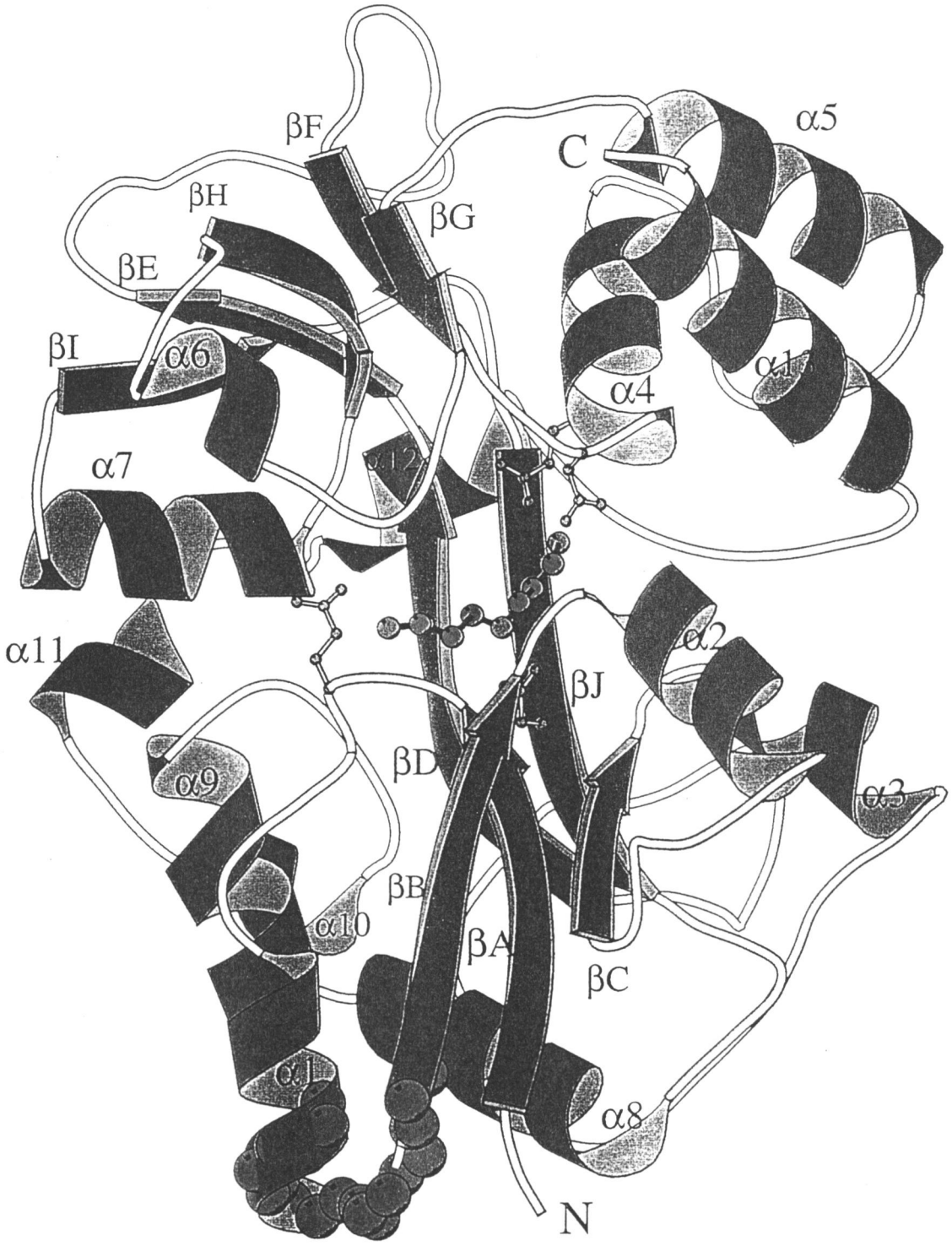

Figure 3.1(B) **Structure of the PotD.**

Ribbon model of the PotD monomer, drawn with the program MOLSCRIPT (44). The N domain lies at the *bottom*, and the C domain is at the *top*. The α helices are *green*, the β strands are *blue*, the coils and loops are *yellow*, and the motif region is *sky blue*. The spermidine molecule is bound to the central cleft between the two domains. The binding site for the spermidine molecule is marked by the side chains of the four acidic residues.

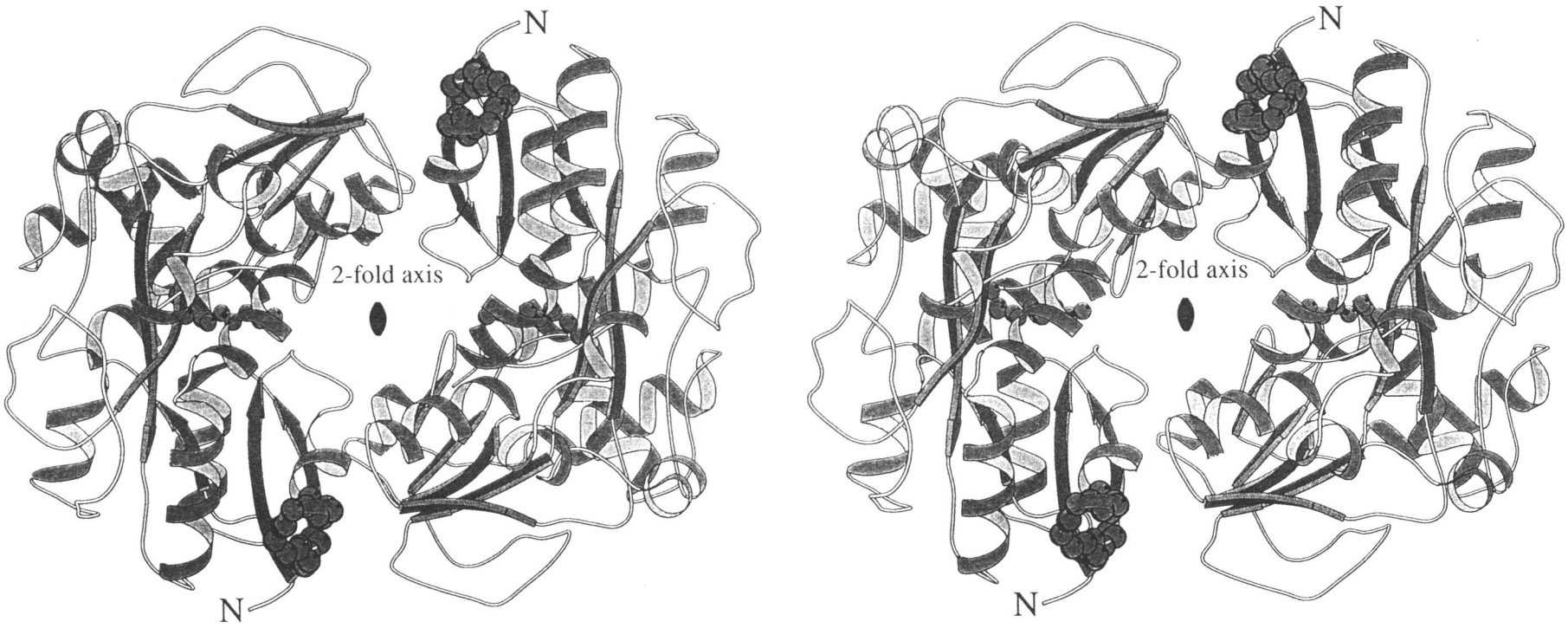

Figure 3.2 Dimeric structure of PotD.

Ribbon drawing of a dimer. Each monomer in a dimer is related by a noncrystallographic 2-fold axis. The spermidine molecule is shown by a *red ball-and-stick model,* and the consensus motif is indicated by *blue balls*. The dimer is primarily stabilized by a network of hydrogen bonds and salt bridges.

There is no substantial difference among the backbone structures of the four independent molecules in the asymmetric unit. Their root mean square (r.m.s.) deviations for the superimposed Cα atoms are as low as 0.40 Å. However, when the Cα atoms of the N and C domains are superimposed separately among the corresponding domains in the asymmetric unit, the C domain shows a larger r.m.s. deviation value (0.42 Å) than the N domain (0.33 Å).

3.4.2 *Subunit Contacts*

The crystal contains two dimeric molecules in the asymmetric unit. The dimensions of the dimer are approximately 70 x 70 x 55 Å. Each monomer in a dimer is related by a noncrystallographic 2-fold axis (Figure 3.2). The r.m.s. deviation values for the Cα atoms between these two related dimers was calculated to be 0.52 Å. The dimerization mainly involves together the interactions between the N domain (βA, α1, and βB) from one monomer and the C domain (α6, α7, and βI) on the other. Consequently, the two clefts in the dimer face each other and cross over the solvent region that is centered around the 2-fold axis. The dimer is stabilized by a network of many hydrogen bonds and van der Waals interactions. In fact, 14 residues participate in direct hydrogen bonds (Tyr30 to Asp141, Gly41 and Glu44 to Gln238, Tyr56 to Gly240 and Thr241, Thr58 to Met219, Glu60 to Glu220, and Asp212 to Asn216 and Glu220). These extensive interactions contribute to the maintenance of the dimer.

3.4.3 *Spermidine Binding*

Crystals of PotD have been grown in the presence of spermidine. Indeed, the omit map at 2.5 Å resolution shows an elongated electron density (Figure 3.3), which is assigned to a spermidine molecule bound to the central cleft between the two domains. The same densities have been found within all four molecules in the asymmetric unit, indicating that the bound spermidine

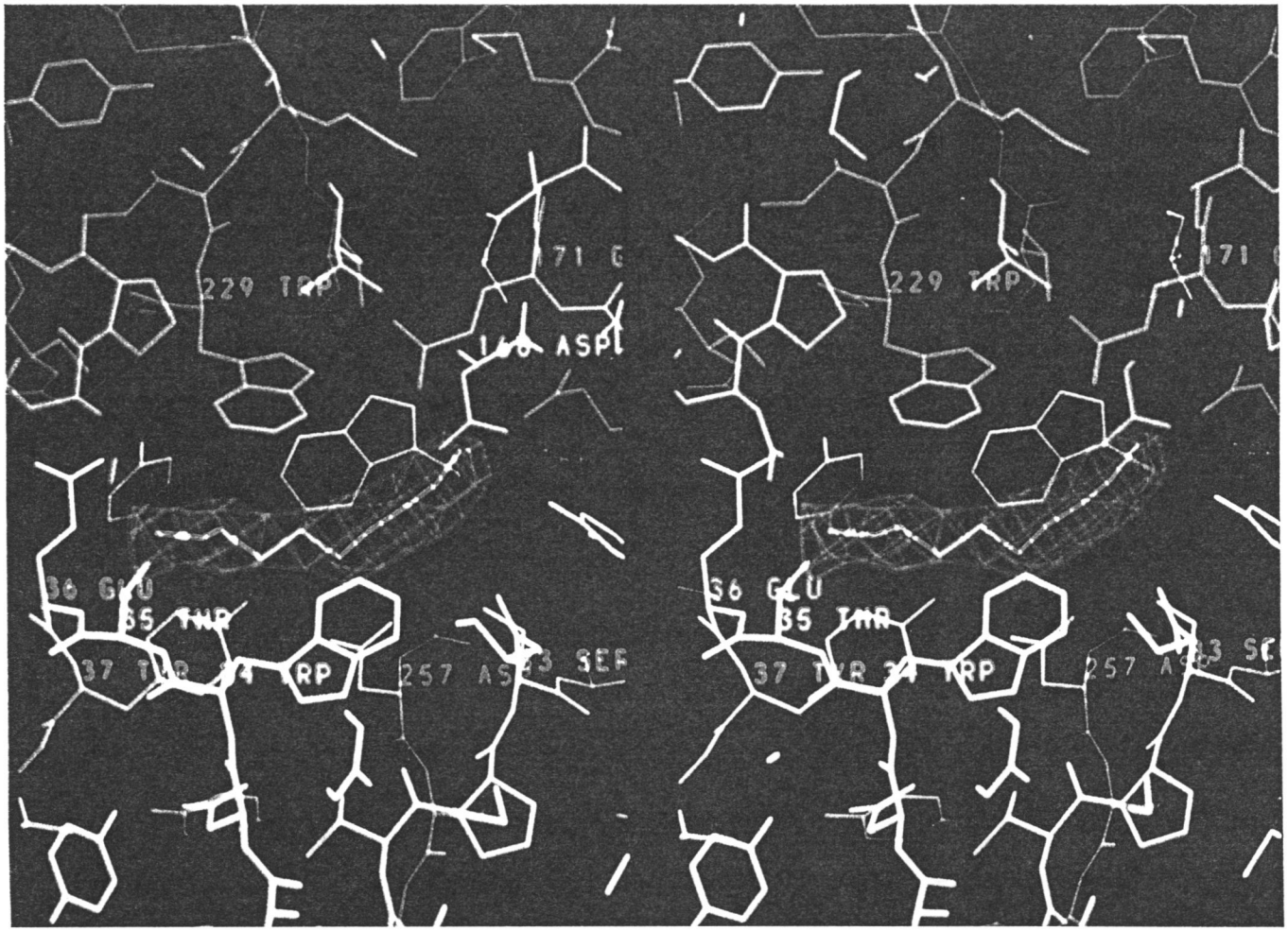

Figure 3.3 Electron density showing the bound spermidine.

Stereo view of the electron density for spermidine in the binding pocket and its environment. The electron density map was calculated with the coefficients $|F_O| - |F_C|$, and the phases from the refined protein and the solvent atoms with the spermidine molecule are omitted. The contour levels are at 3.5σ. The residues of the N domain are *green*, the C domain is *blue*, and the substrate is *red*. The conformation of the bound spermidine and its environment are shown in Figure 3.4.

molecules adopt the identical conformation. Interestingly, the spermidine molecule is bent within the PotD molecule, whereas all kinds of the crystal structures of spermidine in the Cambridge structural database exhibit a linear shape (33,34).

The substrate binding site is located at the middle of the cleft between the two domains. This site forms a hydrophobic box, which is composed of four aromatic side chains, Trp34, Tyr37, Trp255, and Tyr293 in the N domain, and Trp229 in C domain. These aromatic side chains anchor the methylene backbone of the spermidine molecule through van der Waals interactions. The methylene bonds of spermidine are sandwiched between the aromatic side chains of Trp34 and Trp255, which are arranged in parallel (Figure 3.4A). The side chain of Trp229, oriented perpendicular to the previous side chains, covers the spermidine like a lid over the cleft.

Another important feature in the binding site is that four acidic residues, Glu36, Asp168, Glu171, and Asp257, recognize the charged nitrogen atoms of spermidine through numerous ionic interactions (Figure 3.4B). The conformations of these aromatic and acidic residues are conserved well among the four molecules in an asymmetric unit. One terminal amino group of propyl amine moiety in the spermidine forms the salt bridges with the carboxyl side chains of Asp168 and Glu171, and the hydrogen bonds with the side chain of Gln327 and Tyr85. The secondary amino group in the middle is recognized through the side chain of Asp257, and the other terminal amino group forms a salt bridge with the side chain of Glu36 and a hydrogen bond with the side chain of Thr35. These aromatic and acidic side chain atoms embed the spermidine molecule in the cleft so as to prevent no solvent access.

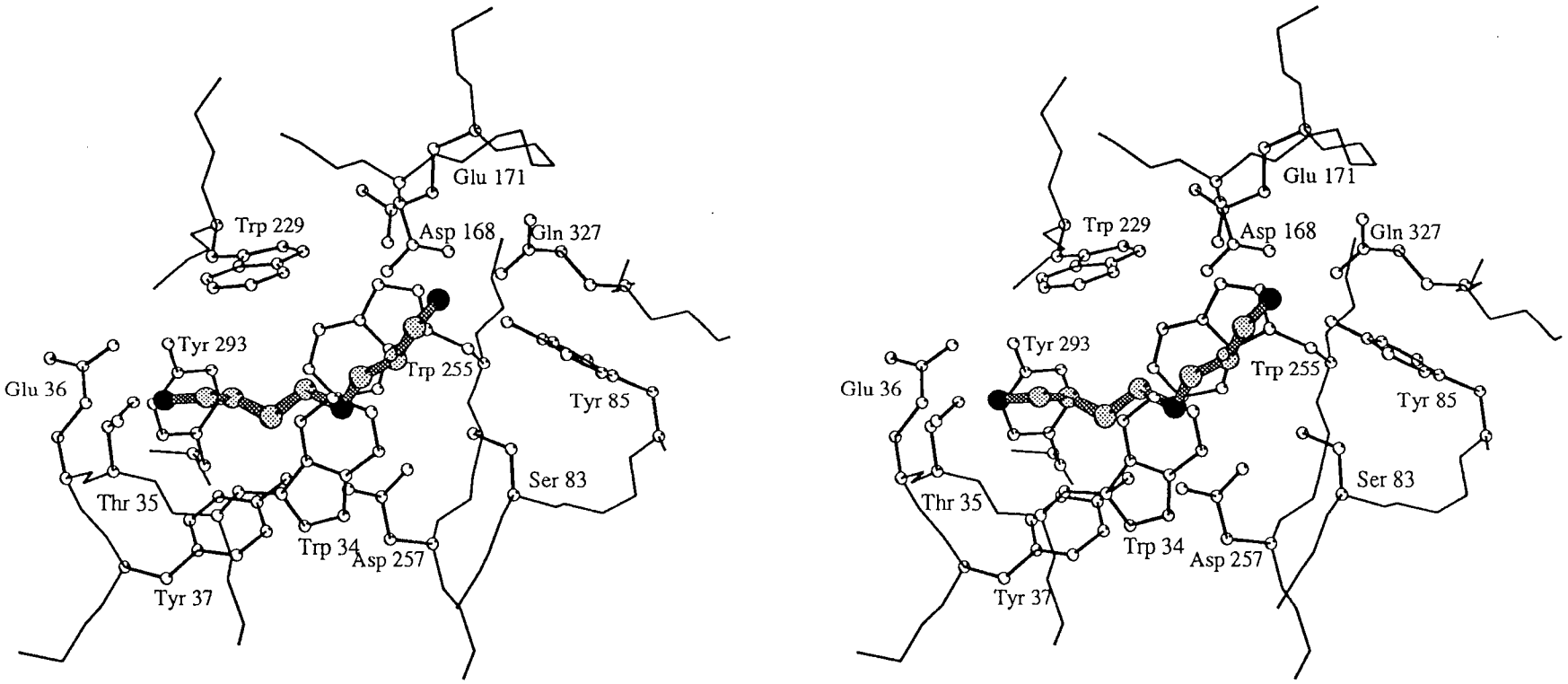

Figure 3.4(A) **Interactions of spermidine with protein atoms.**

A stereo picture showing hydrogen bonds, salt bridges, and van der Waals interactions. Hydrogen bonds and salt bridges are indicated by *dotted lines*. The spermidine molecule is shown by the shadowed *ball-and-stick model*.

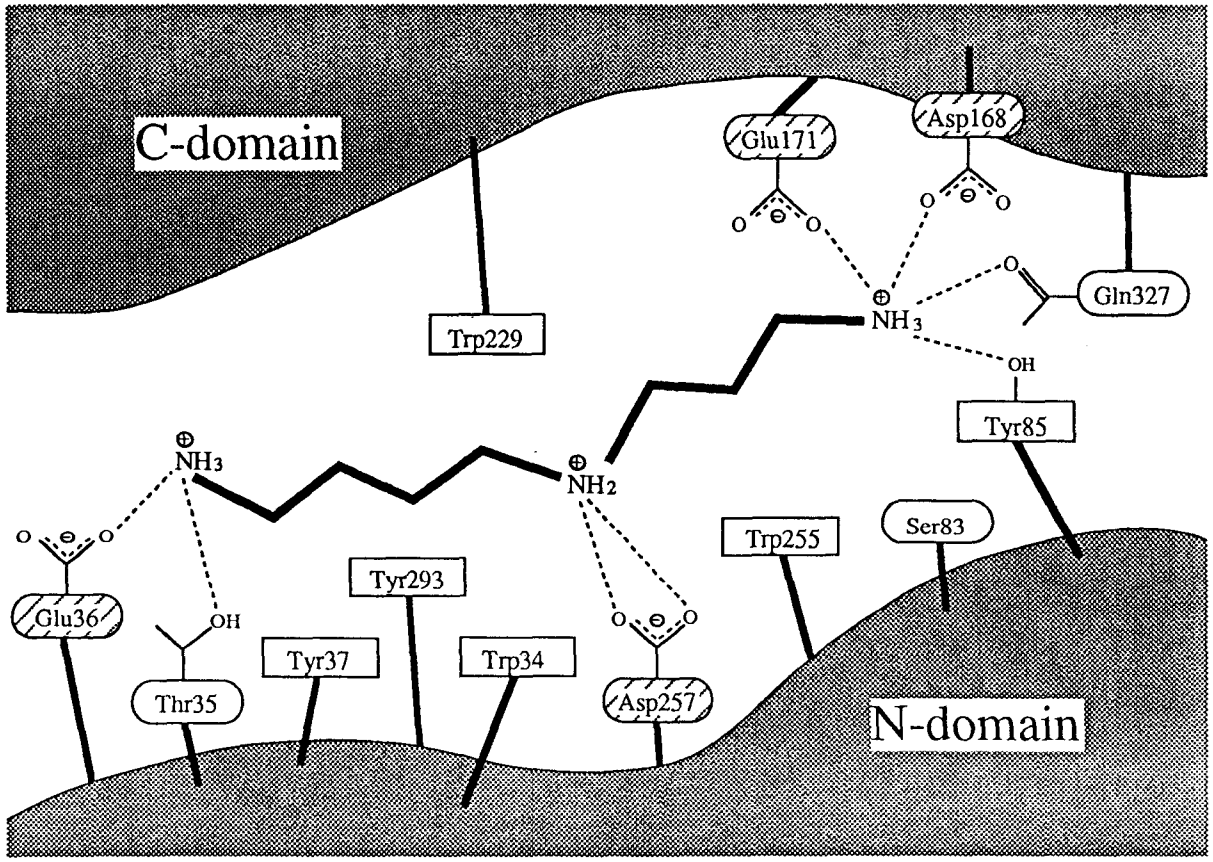

Figure 3.4(B) Interactions of spermidine with protein atoms.

Schematic diagram of hydrogen bonding and van der Waals interactions with spermidine.

3.5 Discussion

3.5.1 *Comparison with Other Periplasmic Binding Proteins*

Among the periplasmic binding proteins, the PotD backbone is most similar to that of MBP from *E. coli*, although their two sequences exhibit an identity less than 20 %. In particular, the similarity between the two N domains is remarkable. When the two domains of PotD are optimally superimposed on the corresponding domains of MBP, the r.m.s. deviation values are evaluated to be 1.64 Å for the 100 Cα atoms between the N domains and 2.63 Å for the 100 Cα positions between the C domains. Furthermore, the active residues of the PotD and MBP proteins can be observed in similar regions of the two topologies (Figure 3.5).

Another notable similarity between the two structures is that a conserved sequence motif is found in both PotD and MBP (35). This conserved sequence motif spans residues 46 - 54 (FTKETGIKV) of PotD, which corresponds to the loop between α1 and βB, and residues 53 - 61 (FEKDTGIKV) of MBP (Figure 3.1). These sequences exhibit a remarkably similar conformation between the two molecules, as proved by the very small r.m.s. deviation value of 0.40 Å for the nine Cα positions.

3.5.2 *Open and Closed Forms*

The crystal structures of MBP have been reported in both states of the open and closed forms (Brookhaven Protein Databank entry 1MBP, closed liganded form; 1OMP, open unliganded form), which correspond to the substrate free form and the complex with the substrate, respectively. Substrate binding induces few conformational changes within each domain. However, it generates a substantial alteration in the relative orientation of the two domains. Substrate binding to MBP yields a hinge bending angle of 35° about an axis

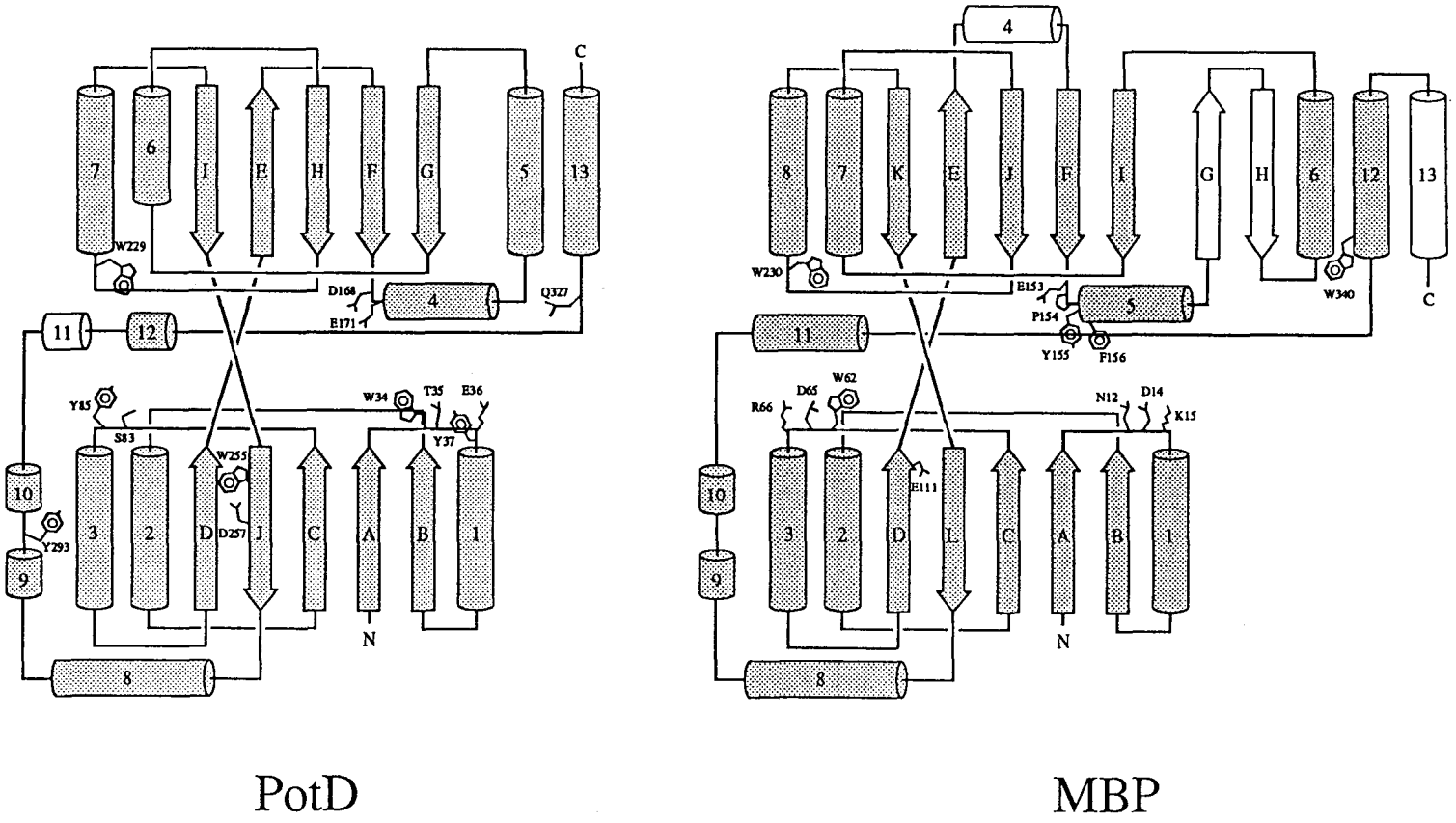

Figure 3.5 Topological diagrams of PotD and MBP.

The α helices are represented as *lettered cylinders*, and the β strands are indicated by *arrows* with *numbers*. Common secondary structure elements between PotD and MBP are *shadowed*. The active residues of the two binding proteins are shown as *solid lines*.

through the central hinge residues (residues 111 and 261) (36). The interdomain orientation of PotD is much closer to the closed form of MBP, indicating that both the PotD and MBP molecules adopt a similar domain arrangement upon binding the substrates (Figure 3.6). These findings suggest that the spermidine bound PotD molecule is the closed form, which presumably is converted from the open, ligand free form.

3.5.3 *Dimer Formation*

The PotD molecule forms a dimer in this crystal structure, although PotD exists as monomeric form in solution, which contains the substrate (data not shown). The ionic interactions between the two subunits are so extensive that they are unlikely to have accidentally taken place during crystallization. All of the crystal structures of the periplasmic binding proteins exhibit monomeric molecules except for a MBP mutant crystal produced in the presence of maltose. This mutant crystal structure revealed a dimeric molecule (36). Furthermore, the MBP protein is purified as a dimer from an *E. coli* strain that is constitutive for the expression of the maltose system and that has been grown in the absence of maltose (37). Therefore, we assume that the switch from the dimer to the monomer of the PotD protein may have physiological significance in polyamine transport.

3.5.4 *Spermidine Recognition*

The residues that participate in the recognition of spermidine spread over the two domains. The N domain comes into more extensive contact with the spermidine through the walls of the hydrophobic box, while the C domain provides the lid of the box. The ligand serves as a pin that links the two domains, and it is completely embedded in the protein atoms that lie between them (Figure 3.4B).

Figure 3.6 Comparison of PotD and MBP.

The PotD molecule (*yellow*) is superimposed on the MBP molecule (*blue*) by matching only the Cα atoms within the N domain. The open form of MBP is shown on the *right*, and the closed form is on the *left*. This view is rotated by 90° about the *vertical* axis in Figure 3.1(B).

The PotD protein can bind putrescine as well as spermidine, although the affinity of putrescine is much lower than that of spermidine. The dissociation constants (K_d) for spermidine and putrescine are 3.2 and 100 μM, respectively (23). These K_d values reflect the spermidine preferential recognition for the primary receptor of the polyamine transport system. The shorter putrescine molecule could possibly make ionic interactions with the acidic residues of Glu36 and Asp257, and form van der Waals interactions with the aromatic residues Trp34, Tyr37, Trp229, Trp255, and Tyr293. These interactions may stabilize the closed conformation. However, the smaller number of interactions, as compared with those with spermidine, would decrease the stability of the closed form.

3.5.5 *Consensus Motif*

The highly conserved sequence motif observed in MBP and PotD suggests a common functional role in the transport system, although mutations introduced in this region of MBP do not clearly cause a transport defect (21,38). When the PotD structure is optimally superimposed onto the MBP structure, the motif is located in the surface loop of the N domain (Figure 3.1), which is distant from the substrate binding site. On the other hand, it is directly connected to the loop between βA and α1, which participates in the substrate binding and is opposite the hinge between the domains. This motif, which also lies on the molecular surface, does not participate in the dimerization. It may be possible that the physiological role of the consensus sequence is to interact with the membrane components, PotB and/or PotC, which could be an initial switch to release the substrate from the protein.

3.5.6 *Interactions with the Membrane Bound Components*

In the course of periplasmic receptor dependent transport, the substrate is initially recognized by a specific binding protein. The subsequent

translocation across the cytoplasmic membrane requires a set of membrane protein components. The membrane-bound components in the polyamine transport machinery are three nonidentical proteins (PotA, -B, and -C). Polyamine uptake appears to be initiated by the formation of a complex between the two membrane-bound components (PotB and PotC) and the periplasmic receptor (PotD). The substrate free PotD protein slightly inhibits spermidine uptake to the cytoplasm (23). This result implies that the closed form of PotD is preferentially recognized by the membrane components.

In spite of many relevant reports (38-43), mutational analyses have not clearly identified the interface of periplasmic binding proteins with their membrane protein components yet. However, it should be noted that the consensus sequence lies in the N domain, which shows a higher similarity of PotD and MBP in terms of the three-dimensional structure. Furthermore, in most of the periplasmic binding proteins including PotD and MBP (Figure 3.5), the folding topology of the N domain is more conserved than the C domain (22). Therefore, it is likely that the interface of PotD with the membrane components is located in the N domain, rather than the C domain.

References

1. Tabor, C. W., and Tabor, H. (1984) *Annu. Rev. Biochem.* **53**, 749-790
2. Pegg, A. E. (1988) *Cancer Res.* **48**, 759-774
3. Kashiwagi, K., Hosokawa, N., Furuchi, T., Kobayashi, H., Sasakawa, C., Yoshikawa, M., and Igarashi, K. (1990) *J. Biol. Chem.* **265**, 20893-20897
4. Kashiwagi, K., Suzuki, T., Suzuki, F., Furuchi, T., Kobayashi, H., and Igarashi, K. (1991) *J. Biol. Chem.* **266**, 20922-20927
5. Kashiwagi, K., Miyamoto, S., Suzuki, F., Kobayashi, H., and Igarashi, K. (1992) *Proc. Natl. Acad. Sci. USA* **89**, 4529-4533
6. Furuchi, T., Kashiwagi, K., Kobayashi, H., and Igarashi, K. (1991) *J. Biol. Chem.* **266**, 20928-20933
7. Pistocchi, R., Kashiwagi, K., Miyamoto, S., Nukui, E., Sadakata, Y., Kobayashi, H., and Igarashi, K. (1993) *J. Biol. Chem.* **268**, 146-152
8. Ames, G. F. L. (1986) *Annu. Rev. Biochem.* **55**, 397-426
9. Furlong, C. E. (1987) in *Escherichia coli* and *Salmonella tryphimurium*: Cellular and Molecular Biology (Neidhardt, F. C., Ingraham, J. L., Low, K. B., Magasanik, B., Schaechter, M., and Umbarger, H. E., eds) pp. 768-796, American Society for Microbiology, Washington, D. C.
10. Kashiwagi, K., Endo, H., Kobayashi, H., Takio, K., and Igarashi, K. (1995) *J. Biol. Chem.* **270**, 25377-25382
11. Kang, C. H., Shin, W. C., Yamagata, Y., Gokcen, S., Ames, G. F. L., and Kim, S. H. (1991) *J. Biol. Chem.* **266**, 23893-23899
12. Oh, B. H., Pandit, J., Kang, C. H., Nikaido, K., Gokcen, S., Ames, G. F. L., and Kim, S. H. (1993) *J. Mol. Biol.* **268**, 11348-11355
13. Sack, J. S., Saper, M. A., and Quiocho, F. A. (1989) *J. Mol. Biol.* **206**, 171-191

14. Sack, J. S., Trakhanov, S. D., Tsigannik, I. H., and Quiocho, F. A. (1989) *J. Mol. Biol.* **206**, 193-207
15. Tame, J. R. H., Murshudov, G. N., Dodson, E. J., Neil, T. K., Dodson, G. G., Higgins, C. F., and Wilkinson, J. A. (1994) *Science* **264**, 1578-1581
16. Pflugrath, J. W., and Quiocho, F. A. (1988) *J. Mol. Biol.* **200**, 163-180
17. Luecke, H., and Quiocho, F. A. (1990) *Nature* **347**, 402-406
18. Quiocho, F. A., and Vyas, N. K. (1984) *Nature* **310**, 381-386
19. Vyas, N. K., Vyas, M. N., and Quiocho, F. A. (1988) *Science* **242**, 1290-1295
20. Mowbray, S. L., and Cole, L. B. (1992) *J. Mol. Biol.* **225**, 155-175
21. Sharff, A. J., Rodseth, L. E., Spurlino, J. C., and Quiocho, F. A. (1992) *Biochemistry* **31**, 10657-10663
22. Spurlino, J.C., Lu, G.-Y., and Quiocho, F.A. (1991) *J. Biol. Chem.* **266**, 5202-5219
23. Kashiwagi, K., Miyamoto, S., Nukui, E., Kobayashi, H., and Igarashi, K. (1993) *J. Biol. Chem.*, **268**, 19358-19363
24. Sugiyama, S., Matsushima, M., Saisho, T., Kashiwagi, K., Igarashi, K., and Morikawa, K. (1996) *Acta Crystallogr.* **D52**, 416-418
25. Steigemann, W. (1974) Ph. D. thesis, Technishe Universität, München.
26. Leslie, A. G. W. (1988) in Proceedings of the Daresbury Study Weekend, 5-6 February 1988 (Bailey, S., Dodson, E., and Phillips, S., eds) pp. 25-31, SERC Daresbury Laboratory, Warrington, United Kingdom
27. Wang, B. C. (1985) *Methods Enzymol.* **115**, 90-112
28. Bricogne, G. (1976) *Acta Crystallogr.* **32**, 832-847
29. Jones, T. A., Zou, J. Y., Cowan, S. W., and Kjeldgaard, M. (1991) *Acta Crystallogr.* **47**, 110-119
30. Brünger, A. T., Kuriyan, J., and Karplus, M. (1987) *Science* **235**,

458-460

31. Jones, T. A. (1978) *J. Appl. Crystallogr.* **11**, 268-272
32. Laskowski, R. A., MacArthur, M. W., Moss, D. S., and Thornton, J. M. (1993) *J. Appl. Crystallogr.* **26**, 283-290
33. Giglio, E., Liquori, A. M., Puliti, R., and Ripamonti, A. (1966) *Acta Cystallogr.* **20**, 683-688
34. Huse, Y. and Iitaka, Y. (1969) *Acta Crystallogr.* **B25**, 498-509
35. Matsuo, Y., and Nishikawa, K. (1994) *FEBS Lett.* **345**, 23-26
36. Sharff, A. J., Rodseth, L. E., Szmelcman, S., Hofnung, M., and Quiocho, F. A. (1995) *J. Mol. Biol.* **246**, 8-13
37. Richarme, G. (1982) *Biochem. Biophys. Res. Commun.* **105**, 476-481.
38. Zhang, Y., Conway, C., Rosato, M., Suh, Y., and Manson, M. (1992) *J. Biol. Chem.* **267**, 22813-22820
39. Duplay, P., Szmelcman, S., Bedouelle, H., and Hofnung, M. (1987) *J. Mol. Biol.* **194**, 663-673
40. Duplay, P., and Szmelcman, S. (1987) *J. Mol. Biol.* **194**, 675-678.
41. Vermersch, P. S., Tesmer, J. J. B., Lemon, D. D., and Quiocho, F. A. (1990) *J. Biol. Chem.*, **265**, 16592-16603
42. Mowbray, S. L. (1992) *J. Mol. Biol.* **227**, 418-440
43. Binnie, R. A., Zhang, H., Mowbray, S., and Hermodson, M. A. (1992) *Protein Sci.* **1**, 1642-1651
44. Kraulis, P. J. (1991) *J. Appl. Crystallogr.*, **24**, 946-950
45. Brünger, A. T. (1992) *Nature* **255**, 472-474
46. Engh, R. A., and Huber, R. (1991) *Acta Crystallogr.* **47**, 392-400

Chapter 4

Spermidine preferential Uptake System in *Escherichia coli*

Identification of Amino Acids Involved in Polyamine Binding in PotD protein

4.1 Abstract

Spermidine binding sites on PotD protein, a substrate binding protein in a periplasm, in the spermidine preferential uptake system in *Escherichia coli* were studied by measuring polyamine transport activities of right-side-out membrane vesicles with mutated PotD proteins prepared through site directed mutagenesis of the *potD* gene and by measuring polyamine binding activities of these mutated PotD proteins. Polyamine transport activities by the mutated PotD proteins paralleled their polyamine binding activities. It was found that Trp34, Thr35, Glu36, Tyr37, Ser83, Tyr85, Asp168, Glu171, Trp229, Trp255, Asp257, Tyr293 and Gln327 of PotD protein were involved in the binding to spermidine. When spermidine uptake activities were measured in intact cells expressing the mutated PotD proteins, it was found that Glu171, Trp255, and Asp257 were more strongly involved in the binding of spermidine to PotD protein than the other amino acids listed above. The dissociation constants of spermidine for the mutated PotD proteins at Glu171, Trp255, and Asp257 increased greatly in comparison with those for the other mutated PotD proteins. Since these three amino acids clearly interact with the diaminopropane moiety of spermidine, the results are in accordance with the finding that PotD protein has a higher affinity for spermidine than for putrescine. Putrescine was found to bind at the position corresponding to the binding site of the diaminobutane moiety of spermidine in PotD protein.

4.2 Introduction

The polyamine content in cells, which plays important roles in cell proliferation and differentiation (1,2), is regulated by polyamine biosynthesis, degradation and transport. /\As for the latter, we obtained and characterized three clones of polyamine transport genes (pPT104, pPT79, and pPT71) in *Escherichia coli* (3). The system encoded by pPT104 is the spermidine preferential uptake system, and that by pPT79 is the putrescine specific uptake system. Furthermore, these two systems are periplasmic transport systems (4, 5), each consisting of four kinds of proteins: the pPT104 clone encoded PotA, PotB, PotC, and PotD proteins, and pPT79 clone encoded PotF, PotG, PotH, and PotI proteins, judging from the deduced amino acid sequences of their nucleotide sequences (6,7). PotD and PotF proteins are periplasmic substrate binding proteins, and PotA and PotG proteins are membrane associated proteins with a nucleotide binding site. PotB and PotC proteins and PotH and PotI proteins are transmembrane proteins that probably form channels for spermidine and putrescine, respectively. Their amino acid sequences in the corresponding proteins are similar to each other. In contrast, the putrescine transport system encoded by pPT71 consists of one membrane protein (PotE protein) with 12 transmembrane segments (8) and is active in the excretion of putrescine from cells through putrescine-ornithine antiporter activity (9). We also found that spermidine uptake by membrane vesicles is strongly dependent on PotD protein, and the uptake by intact cells is completely dependent on ATP through its binding to PotA protein (10). Furthermore, PotA protein was shown to have ATPase activity, and its association with membranes is strengthened by the existence of channel-forming PotB and PotC proteins (11).

Recently, we determined the crystal structure of PotD protein in a complex with spermidine at 2.5-Å resolution (12). It was revealed that four

acidic and five aromatic amino acid residues in PotD protein intact with spermidine (13). In this study, we tried to identify the amino acid residues in PotD protein that are involved in the binding of spermidine by using mutated PotD protein produced by the site-directed mutagenesis of *potD* gene. We found that Glu171, Trp255, and Asp257, among 13 amino acids involved in the interaction with spermidine, are particularly important in the recognition.

4.3 Material and method

4.3.1 *Bacterial Strains, Plasmids, and Culture Conditions*

A polyamine-requiring mutant, *E. coli* DR112 (14), provided by Dr. D. R. Morris (University of Washington), was grown as described previously (15). *E. coli* TG1 (*Δ(lac-pro), supE, thi, hsdD5/* F'*traD36,proA*$^+$*B*$^+$, *lacI*^{q}, *lacZ*Δ*M15*), which has a higher transformation efficiency, was grown in 2YT medium (16). A spermidine transport- and polyamine biosynthesis-deficient mutant MA261 *potD::Km* (10) was grown in medium A in the absence of polyamines as described previously (17). Plasmids pPT86 containing *potABC* gene and pUC*potD* were prepared as described previously (10). Plasmid pMW*potD* was prepared by inserting the 1.7 kilobase *Eco*RI-*Hind* III fragment of pUC*potD* into the same restriction site of pMW119 (18). Transformation of *E. coli* cells with plasmids was carried out as described by Maniatis *et al.* (19). Appropriate antibiotics (30 μg/ml chloramphenicol, 100 μg/ml ampicillin, and 50 μg/ml kanamycin) were added during the culture of *E. coli* cells.

4.3.2 *Mutagenesis of potD Gene*

To prepare *potD* mutants, a 1.7 kilobase *Eco*RI-*Hind*III fragment of pUC*potD* was inserted into the same site of M13mp19 (20). Site-directed mutagenesis was carried out by the method of Sayers *et al.* (21) with a

Sculptor™ *in vitro* mutagenesis system (Amersham Corp.), using the oligonucleotides shown in Table 4.1. The mutated DNA fragments were isolated from the replicative from of M13 and religated into the same site of pUC*potD*. Mutations were confirmed by DNA sequencing (22) using the M13 phage system (20) with commercial and synthesized primers.

Table 4.1

Oligonucleotides used for the site-directed mutagenesis of the *potD* gene

Mutant	Primer sequence
W34L	CGT ACT CGG TC**A** AGT TGT AGA AA
T35A	CAC GTA CTC GG**C** CCA GTT GTA GA
E36Q	GGC ACG TAC T**G**G GTC CAG TTG
Y37A	CTG GCG GCA CG**G** CCT CGG TCC AGT
S83A	GTA ATA GGT TG**C** AGG AAC CAC CA
Y85A	TAT CAA CGT AA**G** CGG TTG AAG GAA
Y86A	TTT TAT CAA CG**G** CAT AGG TTG AAG
D168N	TCA CGG GCA T**T**G TCG GTC AAC
R170L	GGA ACA CTT CA**A** GGG CAT CGT CG
E171Q	TGG AAC ACT T**G**A CGG GCA TCG
W229L	AGA ACC GTT C**A**A GAT CAT GCC
W255L	GCT GTC CAT C**A**A GAA AAT GCC
D257N	GCC AGG CTG T**T**C ATC CAG AAA
D257E	ATC GCC AGG CT**C** TCC ATC CAG AA
Y293A	TTG GCG TTG GA**G** CAC CGA TAG TTT
Q327A	CAA CGT CAT TC**G** CCC ATT CGC CAT

The mutanted nucleotides are underlined.

4.3.3 *Polyamine Uptake by Right-side-out Membrane Vesicles*

Right-side-out membrane vesicles were prepared from *E. coli* DR112/pPT86 as described previously (23). Periplasmic proteins were obtained from *E. coli* TG1 containing pUC*potD*- or pUC- mutated *potD* according to the method of Oliver and Beckwith (24). PotD protein occupied ~60 % of the total periplasmic proteins, and they were used for the PotD protein source. The reaction mixture (0.1 ml: containing 20 mM potassium phosphate buffer (pH 6.6), 50 mM HEPES/KOH (pH 7.6), 5 mM $MgSO_4$, 20 mM D-lactate (lithium salt), 100 μg membrane vesicles protein, 70 μg of PotD or mutated protein, and 20 μM [^{14}C]putrescine (4.07 GBq/mmol) or 4 μM [^{14}C]spermidine (4.07 GBq/mmol), was incubated at 37 。C for 10 min. Membrane vesicles were collected on membrane filters (cellulose acetate, 0.45 μm; Advantec Tokyo), and the radioactivity was counted with a liquid scintillation spectrometer. Protein content was measured by the method of Lowry *et al.* (25).

4.3.4 *Assay for Polyamine Binding to PotD Protein*

The reaction mixture (0.1 ml: containing 10 mM Tris-HCl (pH 7.5), 30 mM KCl, and a combination of 10 μg of PotD protein and 4 μM [^{14}C]spermidine (2.03 GBq/mmol) or either 100 μg of PotD protein or 35 μM [^{14}C]putrescine (4.07 GBq/mmol)), was incubated at 30 。C for 5 min. PotD protein was collected on membrane filters (cellulose nitrate, 0.45 μm; Advantec Tokyo), and the radioactivity was counted with a liquid scintillation spectrometer. The dissociation constant (Kd) and the number of binding sites (B_{max}) of spermidine for PotD protein were calculated from a Scatchard plot (26) by changing the substrate concentrations from 1 to 50 μM.

4.3.5 *Spermidine Uptake by Intact Cells*

E. coli MA261 *potD::Km* containing pMW*potD*- or pMW-mutated *potD* was grown in medium A until A_{540} reached 0.3. The assay for spermidine uptake was performed as described previously (23), except that 1 μM (4.07 GBq/mmol) or 10 μM (370 MBq/mmol) [^{14}C]spermidine was used as substrate.

4.4 Results

4.4.1 *Spermidine and Putrescine Uptake Activities by Right-side-out Membrane Vesicles and Mutated PotD Protein*

Recently, we determined the tertiary structure of PotD protein in a complex with spermidine by X-ray crystallographic analysis (13). Figure 4.1*A* shows 13 amino acids (Trp34, Thr35, Glu36, Tyr37, Ser83, Tyr85, Asp168, Glu171, Trp229, Trp255, Asp257, Tyr293 and Gln327) that may be involved in the spermidine binding. In addition, it has been reported that Tyr86 and Arg170 might also participate in the spermidine binding from the prediction of the structural similarity between PotD protein and maltodextrin binding protein (27). Therefore, we prepared PotD proteins mutated at the 15 amino acids listed above by site directed mutagenesis of *potD* gene (Table 4.1) and analyzed the activities of the mutated PotD proteins by three different assay methods.

First, spermidine and putrescine uptake activities were measured using right-side-out membrane vesicles and PotD or mutated PotD protein. Right-side-out membrane vesicles were prepared from *E. coli* DR112/pPT86, in which relatively large amounts of PotA, PotB, and PotC proteins are synthesized (6). Periplasmic protein prepared from *E. coli* TG1/pUC*potD* was used as the source of PotD and mutated PotD protein. Spermidine uptake activities decreased greatly with mutated PotD proteins (W255L and D257N)

A

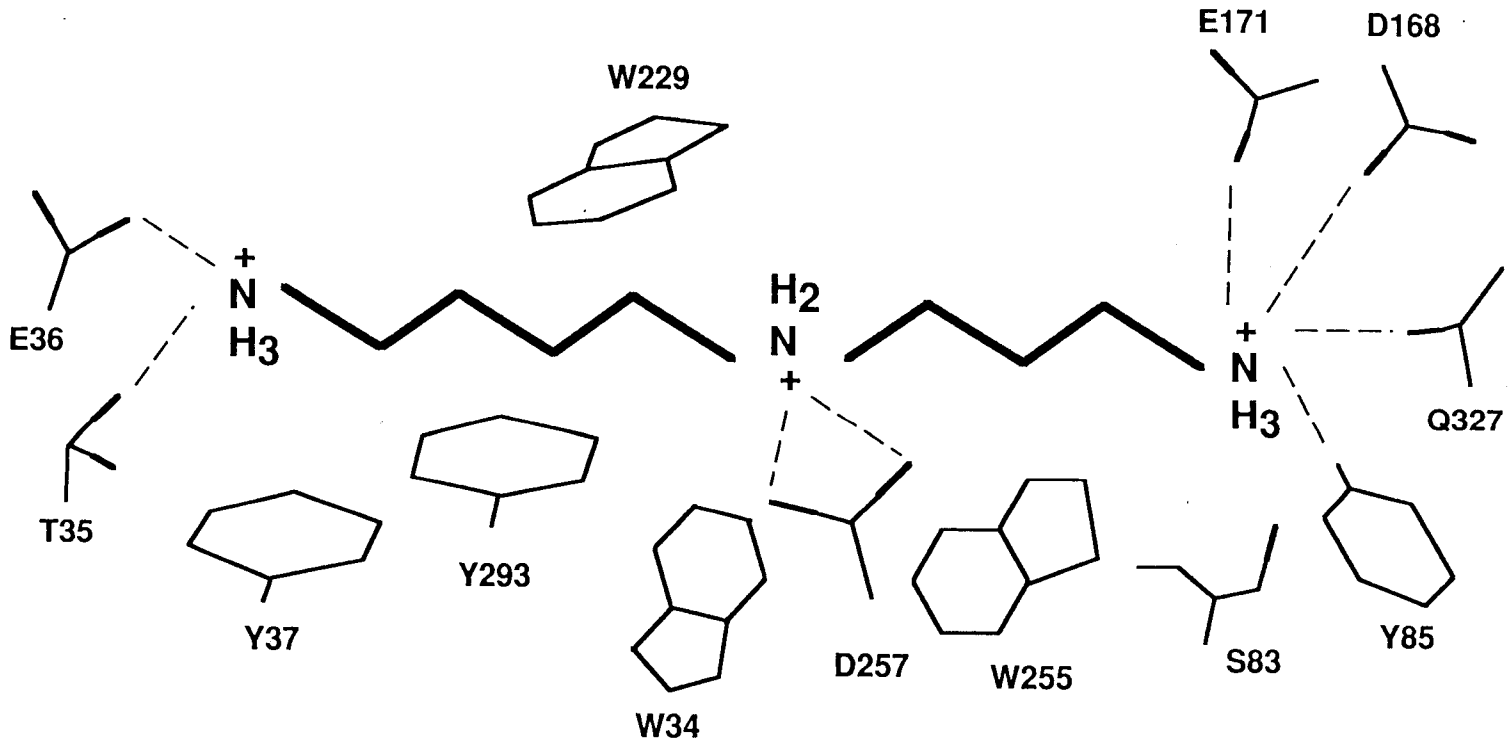

Figure 4.1

Polyamine uptake by right-side-out membrane vesicles and mutated PotD protein and polyamine binding to mutated PotD protein.

A, the 13 amino acids of PotD protein excepted to be involved in the interaction with spermidine.

B

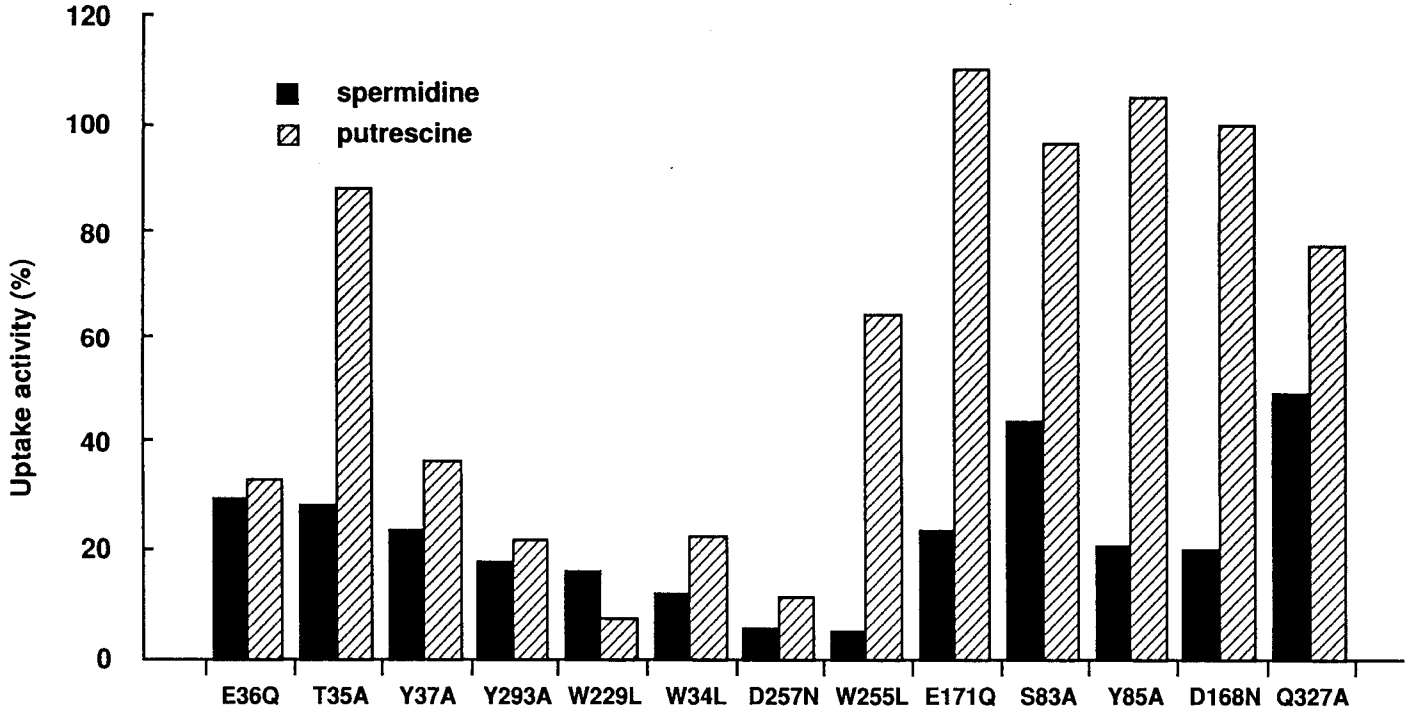

Figure 4.1

Polyamine uptake by right-side-out membrane vesicles and mutated PotD protein and polyamine binding to mutated PotD protein.

B, Polyamine uptake. Control activities (100 %) with normal PotD protein for spermidine (■) and putrescine (▨) uptake were 24.6 and 4.8 pmol/min/mg protein, respectively.

C

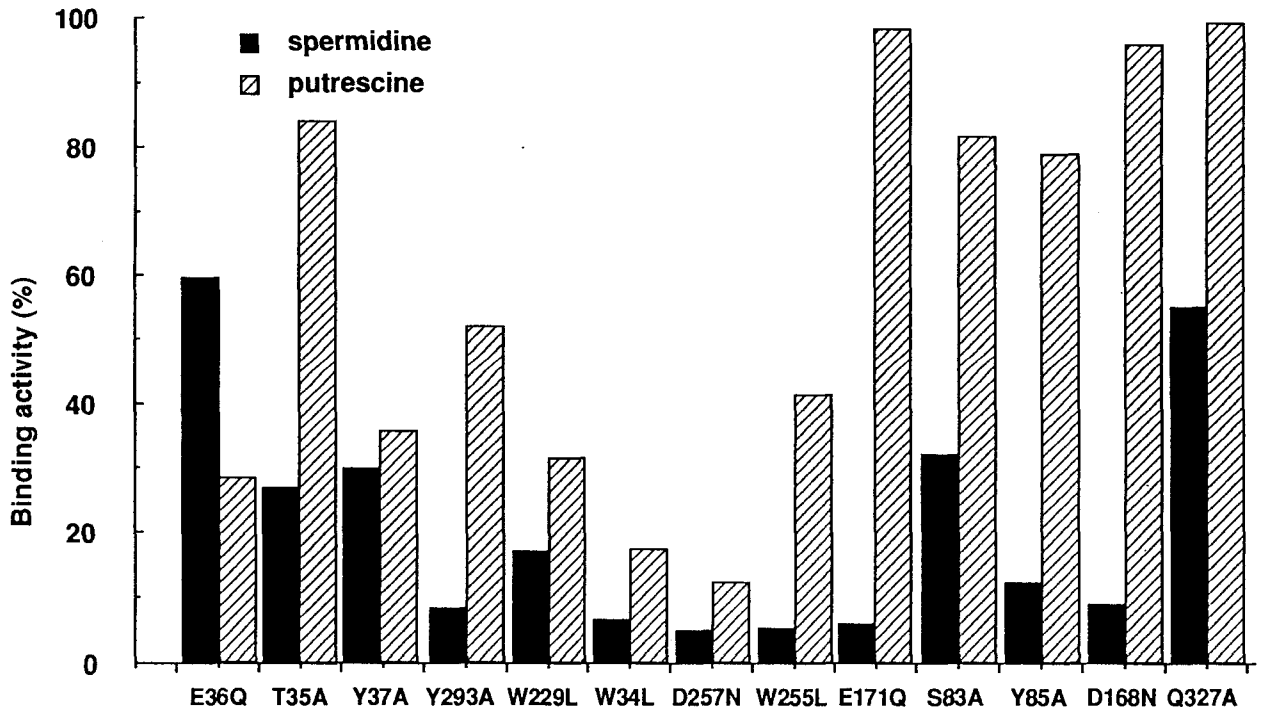

Figure 4.1

Polyamine uptake by right-side-out membrane vesicles and mutated PotD protein and polyamine binding to mutated PotD protein.

C, Polyamine binding. Control activities (100 %) with normal PotD protein for spermidine (■) and putrescine (▨) binding were 7.31 and 0.42 nmol/mg protein, respectively. Each value is the average of duplicate determinations.

in which a closely located amino acid or one interacting with the secondary amine of spermidine is modified (Figure 4.1*B*). The activity also decreased with all mutated PotD proteins (E36Q, T35A, Y37A, Y293A, W229L, W34L, E171Q, S83A, D168N, and Q327A) whose amino acids were strongly suggested to be involved in the binding of spermidine by X-ray analysis. Spermidine uptake activities with other mutated PotD proteins (Y86A and R170L) did not change significantly (data not shown).

Putrescine uptake activity greatly decreased with certain mutated PotD proteins (E36Q, Y37A, Y293A, W34L, and D257N) in which an amino acid interacting with the diaminobutane moiety of spermidine is modified (Figure 4.1*B*). The activity did not significantly decrease with other mutated PotD proteins (E171Q, Y85A, and D168N) in which an amino acid interacting with the aminopropyl moiety of spermidine is modified. The mutated PotD protein W255L slightly decreased the activity. The results indicate that putrescine occupies the position corresponding to the binding site of the diaminobutane moiety of spermidine in PotD protein. It should also be noted that the substitution of Thr35, which was involved in the binding of spermidine, was not connected with the interaction with putrescine.

4.4.2 *Spermidine and Putrescine Binding to Mutated PotD protein*

Polyamine binding to PotD protein was measured using 4 μM spermidine or 35 μM putrescine as substrate. As shown in Figure 4.1C, the amounts of spermidine bound to the mutated PotD proteins almost paralleled the spermidine uptake activities of the proteins except for the E36Q mutated protein. The release of spermidine from this mutated protein may be slower than that from the others. Putrescine binding was measured using a 10 times greater amount of mutated PotD protein since the affinity for putrescine (K_d = 100 μM) is much lower than that for spermidine (K_d = 3.2 μM) (7). The amounts of putrescine bound to the mutated PotD proteins also almost

paralleled the putrescine uptake activities of the proteins. Since the W255L mutated protein significantly decreased both the putrescine uptake and binding activities, Trp255 may also be involved in the interaction with the primary amine of putrescine, which corresponds to the secondary amine of spermidine.

4.4.3 *Spermidine Uptake Activities of Intact Cells Containing Mutated PotD Proteins*

Spermidine uptake activities were measured with *E. coli* MA261 *potD::Km* containing pMW-mutated *potD*, in which the expression of PotD or mutated PotD protein was about four times greater than that in wild-type MA261 cells. The activity with intact cells was measured with 1 or 10 μM spermidine, as the K_m value for spermidine is 0.1 μM (3); it was observed to be much greater than that with right-side-out membrane vesicles and PotD protein. One reason for this was that the possibility of PotD protein interaction with the channel-forming PotB and PotC proteins was increased by the existence of the outer membrane. When the activity was measured in intact cells, the difference among the activities of the mutated PotD proteins became more pronounced. As shown in Table 4.2, Asp257 was the most important amino acid for recognition of spermidine, with Trp255 and Glu171 also being strongly involved. Other mutated PotD proteins slightly decreased the spermidine uptake activity, but the mutated PotD protein S83A did not. Replacement of Asp257 by Glu resulted in uptake activity at 70 % of normal PotD protein, indicating that a negative charge at position of 257 is important (data not shown).

The dissociation constants (K_d) and the number of binding sites (B_{max}) of spermidine for the mutated PotD proteins were then measured. Since the B_{max} value (1 mol/PotD protein) did not change significantly, the change in binding affinity was mainly due to the change in the K_d values. As shown in Table 4.2, the K_d value of spermidine for normal PotD protein was estimated

Table 4.2

Binding affinity for spermidine of the mutanted PotD proteins and spermidine uptake activity in intact cells containing pMW-mutated PotD

PotD protein	Binding affinity[a] *Kd*	Spermidine uptake activity[a]	
		1 μM[b]	10 μM[b]
	μM	*pmol / min / mg protein (%)*	
Normal	3.7	645 (100)	657 (100)
W34L	49	387 (60)	528 (80)
T35A	15	497 (77)	524 (80)
E36Q	9.9	386 (60)	407 (62)
Y37A	13	297 (46)	415 (63)
S83A	6.7	522 (81)	618 (94)
Y85A	33	502 (78)	645 (98)
D168N	38	332 (52)	616 (94)
E171Q	>500	5.5 (0.9)	84.1 (13)
W229L	10	522 (81)	618 (94)
W255L	>500	16.8 (2.6)	176 (27)
D257N	>500	3.2 (0.5)	17.7 (2.7)
Y293A	75	355 (55)	611 (93)
Q327A	6.8	503 (78)	657 (100)

[a] Each value is the average of duplicate determinations.

[b] This is the spermidine concentration used as substrate in the uptake assay.

to be 3.7 μM. However, the K_d values of spermidine for the three mutated proteins D257N, W255L, and E171Q increased greatly, paralleling the decreased in spermidine uptake activities of intact cells. We previously reported that the concentration of spermidine-PotD protein in the periplasm would be ~3.1 μM if the spermidine concentration was 0.1 μM under standard conditions (10).

The amino acids involved in the recognition of spermidine are summarized in Figure 4.2. There were four acidic amino acids, three tyrosines, three tryptophans, and one molecule each of serine, threonine, and glutamine, and they were classified into three groups: most strongly involved, Asp257, Glu171, and Trp255; moderately involved, Asp168, Trp34, Trp229, Tyr85, and Tyr293; and weakly involved, Glu36, Tyr37, Thr35, Ser83, and Gln327.

4.5 Discussion

The spermidine preferential uptake system belongs to the ATP binding cassette (ABC) superfamily (4, 5). The tertiary structures of several periplasmic substrate binding proteins in the ATP binding cassette superfamily have been characterized by X-ray crystal structure analysis (28-31). The structural similarity among substrate binding proteins is striking. There are two globular domains connected by short peptide segments. Between the domains lies a large cleft that binds the substrate. Furthermore, structure/function analysis of histidine binding protein was performed with several mutated histidine binding proteins (32, 33). In the case of PotD protein, it was suggested by X-ray crystal structural analysis(13) that 13 amino acids may be involved in the interaction with spermidine.

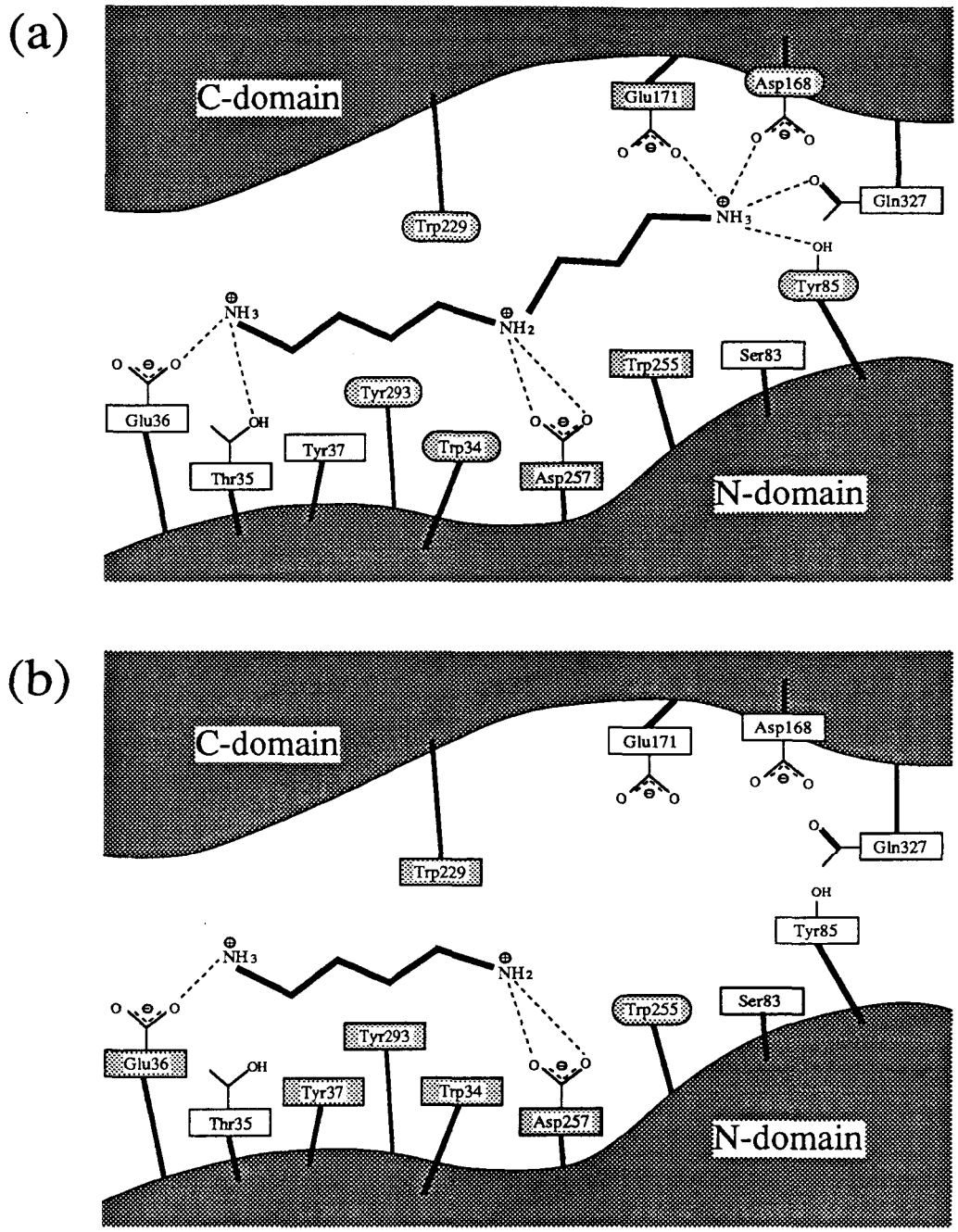

Figure 4.2 Binding site of PotD protein.

(a) Spermidine binding site. *Shaded boxes*, most strongly involved amino acid; *Shaded ovals*, moderately involved amino acid; *white boxes*, weakly involved amino acid. (b) Predicted binding site. *Shaded boxes*, most strongly involved amino acid; *Shaded ovals*, moderately involved amino acid.

In this study, we tried to identify the amino acids that are involved in the binding of spermidine by measuring spermidine uptake activities of right-side-out membrane vesicles and intact cells with mutated PotD proteins as well as spermidine binding activities of mutated PotD proteins. We found that amino acids, especially Glu171, Trp255, and Asp257, involved in the interaction with the diaminopropane moiety of spermidine, are more crucial in the binding of spermidine to PotD protein than those involved in the interaction with the aminobutyl moiety of spermidine. Putrescine was found to bind at the position corresponding to the binding site of the diaminobutane moiety of spermidine in PotD protein (Figure 4.2B). These results explain why spermidine has a higher affinity for PotD protein than putrescine. Among the above three amino acids, Asp257, which interacts with the secondary amine of spermidine, is most strongly involved in the binding to spermidine. In this connection, it should be noted that the secondary amine of spermidine or spermine most effectively contributes to the interaction with tRNA (34).

The putrescine-specific uptake system encoded by pPT79 also belongs to the ATP binding cassette superfamily (7), and PotF protein is a substrate binding protein that exists in periplasm. The amino acid sequences of PotD and PotF proteins exhibit 35 % homology, indicating that the two proteins have similar three-dimensional structures (Figure 4.3). However, Tyr85, Trp255, and Gln327, which are involved in the interaction with the aminopropyl moiety of spermidine, are missing at the equivalent position of PotF protein. On the other hand, Trp34, Tyr37, Trp229, Asp257, and Trp293, which recognize the diaminobutane moiety of spermidine, exist at the equivalent position in PotF protein. In PotF protein, Thr35 and Glu36, which also recognize the diaminobutane moiety of spermidine, were replaced by Ser and Asp, respectively. The affinity of PotF protein for putrescine was stronger than that of PotD protein (7, 10). Since the side chains of Ser and Asp are smaller than those of Thr and Glu, putrescine may be accommodated easily

into the cleft between the N- and C-terminal domains of PotF protein. In this regard, it should be noted that Thr35 of PotD protein was involved in the recognition of spermidine, but not putrescine.

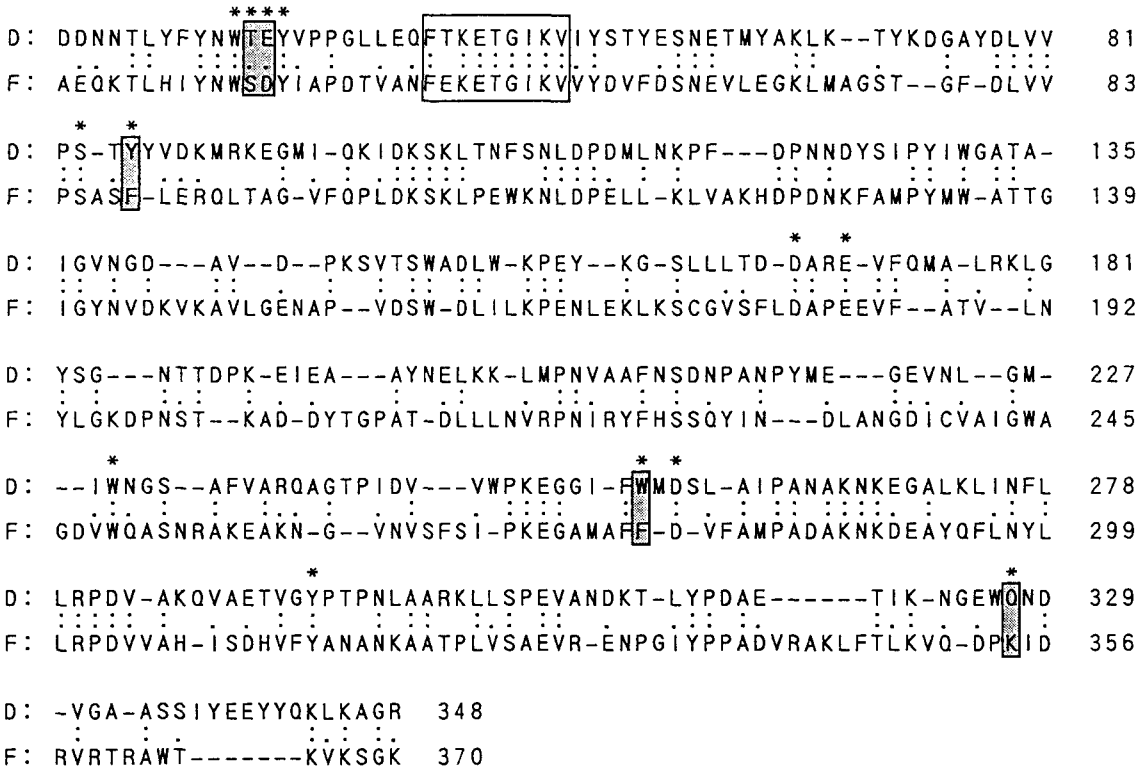

Fig. 4.3 Comparison of amino acid sequences between PotD and PotF proteins.

Asterisks indicate the amino acids involved in the interaction with spermidine; *shaded boxes* differences in the amino acids involved in the interaction with spermidine; Identical amino acids are indicated by *colons*, and equivalent amino acids by *periods*.

References

1. Tabor, C. W., and Tabor, H. (1984) *Annu. Rev. Biochem.* **53**, 749-790
2. Pegg, A. E. (1988) *Cancer Res.* **48**, 759-774
3. Kashiwagi, K., Hosokawa, N., Furuchi, T., Kobayashi, H., Sasakawa, C., Yoshikawa, M., and Igarashi, K. (1990) *J. Biol. Chem.* **265**, 20893-20897
4. Ames, G. F. L. (1986) *Annu. Rev. Biochem.* **55**, 397-426
5. Higgins, C. F. (1995) *Cell* **82**, 693-696
6. Furuchi, T., Kashiwagi, K., Kobayashi, H., and Igarashi, K. (1991) *J. Biol. Chem.* **266**, 20928-20933
7. Pistocchi, R., Kashiwagi, K., Miyamoto, S., Nukui, E., Sadakata, Y., Kobayashi, H., and Igarashi, K. (1993) *J. Biol. Chem.* **268**, 146-152
8. Kashiwagi, K., Suzuki, T., Suzuki, F., Furuchi, T., Kobayashi, H., and Igarashi, K. (1991) *J. Biol. Chem.* **266**, 20922-20927
9. Kashiwagi, K., Miyamoto, S., Suzuki, F., Kobayashi, H., and Igarashi, K. (1992) *Proc. Natl. Acad. Sci. USA* **89**, 4529-4533
10. Kashiwagi, K., Miyamoto, S., Nukui, E., Kobayashi, H., and Igarashi, K. (1993) *J. Biol. Chem.*, **268**, 19358-19363
11. Kashiwagi, K., Endo, H., Kobayashi, H., Takio, K., and Igarashi, K. (1995) *J. Biol. Chem.* **270**, 25377-25382
12. Sugiyama, S., Matsushima, M., Saisho, T., Kashiwagi, K., Igarashi, K., and Morikawa, K. (1995) *Acta Crystallogr.* **D52**, 416-418
13. Sugiyama, S., Vassylyev, D. G., Matsushima, T., Kashiwagi, K., Igarashi, K., and Morikawa, K. (1996) *J. Biol. Chem.* **271**, 9519-9525
14. Linderoth, N., and Morris, D. R. (1983) *Biochem. Biophys. Res. Commun.* **117**, 616-622
15. Kashiwagi, K., and Igarashi, K. (1988) *J. Bacteriol.* **170**, 3131-3135

16. Sambrook, J., Fritsch, E. F., and Maniatis, T. (1989) *Molecular Cloning, A Laboratory Manual*, pp.A1-A3 and A12-A13, Cold Spring Harbor Laboratory Press, Cold Spring Harbor. NY
17. Kashiwagi, K., Yamaguchi, Y., Sakai, Y., Kobayashi, H., and Igarashi, K. (1990) *J. Biol. Chem.* **265**, 8387-8391
18. Yamaguchi, K., and Masamune, Y. (1985) *Mol. & Gen. Genet.* **200**, 362-367
19. Maniatis, T., Fritsch, E. F., and Sambrook, J. (1989) *Molecular Cloning, A Laboratory Manual*, pp.250-251, Cold Spring Harbor Laboratory Press, Cold Spring Harbor. NY
20. Yanisch-Perron, C., Vieira, J., and Messing, J. (1985) *Gene (Amst.)* **33**, 103-119
21. Sayers, J. R., Krekel, C., and Eckstein, F. (1992) *Biotechniques* **13**, 592-596
22. Sanger, F., Nicklen, S., and Coulson, A.E. (1977) *Proc. Natl. Acad. Sci. U. S. A.* **74**, 5463-5467
23. Kashiwagi, K., Kobayashi, H., and Igarashi, K. (1986) *J. Bacteriol.* **165**, 972-977
24. Oliver, D. B., and Beckwith, J. (1982) *Cell* **30**, 311-319
25. Lowry, O. H., Rosebrough, N. J., Farr, A. L., and Randall, R. J. (1951) *J. Biol. Chem.* **193**, 265-275
26. Scatchard, G. (1949) *Ann. N. Y. Acad. Sci.* **84**, 4767-4771
27. Matsuo, Y., and Nishikawa, K. (1994) *FEBS Letters* **345**, 23-26
28. Adams, M. D., and Oxender, D. L. (1989) *J. Biol. Chem.* **264**, 15739-15742
29. Yao, N., Trakhanov, S., and Quiocho, F. A. (1994) *Biochemistry* **33**, 4769-4779
30. Oh, B., Kang, C., De Bondt, H., Kim, S., Nikaido, K., Joshi, A. K., and Ames, G. F. L. (1994) *J. Biol. Chem.* **269**, 4135-4143

31. Oh, B., Ames, G.F.-L., and Kim, S. (1994) *J. Biol. Chem.* **269**, 26323-26330

32. Wolf, A., Shaw, E.W., Nikaido, K., and Ames, G.F.-L. (1994) *J. Biol. Chem.* **269**, 23051-23058

33. Wolf, A., Shaw, E.W., Oh, B., De Bondt, H., Joshi, A.K., and Ames, G.F. -L. (1995) *J. Biol. Chem.* **270**, 16097-16106

34. Frydman, L., Rossomando, P.C., Frydman, V., Fernandez, C.O., Frydman, B., and Samejima, K. (1992) *Proc. Natl. Acad. Sci. U. S. A.* **89**, 9186-9190

Chapter 5

The 1.8 Å X-ray structure of the *Escherichia coli* PotD protein complexed with spermidine and the characteristics of polyamine binding site

5.1 Abstract

The PotD protein from *Escherichia coli* is one of the components of the polyamine transport system present in the periplasm. This component specifically binds either spermidine or putrescine. The crystal structure of the *E. coli* PotD protein complexed with spermidine was solved at 1.8 Å resolution and revealed the detailed substrate binding mechanism. The structure provided the detailed conformation of the bound spermidine. Furthermore, a water molecule was clearly identified in the binding site lying between the amino-terminal domain and carboxyl-terminal domain. Through this water molecule, the bound spermidine molecule forms two hydrogen bonds with Thr35 and Ser211. Another periplasmic component of polyamine transport, the PotF protein, exhibits 35% sequence identity with the PotD protein, and it binds only putrescine, and not spermidine. To understand these different substrate specificities, model building of the PotF protein was performed on the basis of the PotD crystal structure. The hypothetical structure suggests that the side chain of Lys349 in PotF inhibits spermidine binding because of the repulsive forces between its positive charge and spermidine. On the other hand, putrescine could be accommodated into the binding site without any steric hindrance because its molecular size is much smaller than that of spermidine, and the positively charged amino group is relatively distant from Lys349.

5.2 Introduction

Polyamines, such as putrescine, spermidine, and spermine, are linear aliphatic biogenic molecules with two or more positively charged amino groups. They are involved in a wide variety of biological reactions, including nucleic acid and protein synthesis (1,2).

The polyamine transport genes in *Escherichia coli* have been cloned and characterized (3-7). The proteins encoded by pPT104 and pPT79 operons constitute the spermidine-preferential and the putrescine-specific uptake system, respectively (8,9). Each polyamine transport system consists of four proteins: pPT104 encodes the PotA, -B, -C, and -D proteins, and pPT79 encodes the PotF, -G, -H, and -I proteins. PotA and PotG are bound to the inner surface of the cytoplasmic membrane. PotB, -C, -H, and -I are transmembrane components that probably form polyamine transport channels. PotD and PotF are periplasmic components. PotD binds both spermidine and putrescine, although spermidine is preferred (6). In contrast, PotF binds only putrescine (7).

The crystal structure of the PotD protein complexed with spermidine was previously determined at 2.5 Å resolution (10). The structure was found to be very similar to those of other periplasmic substrate-binding proteins, such as arabinose- (ABP) (11), galactose/glucose- (GGBP) (12), leucine- (LBP) (13), leucine/isoleucine/valine- (LIVBP) (14), maltodextrin- (MBP) (15,16), sulfate- (SBP) (17), and lysine/arginine/ornithine- (LAO) (18,19) binding proteins, with repeating β-α-β units (16,20), although PotD shows no significant overall sequence similarity with any of them. In particular, its overall folding topology is the same as those of MBP, SBP, and LAO. The detailed structural comparison has been published elsewhere (10). The 2.5 Å X-ray structure of the PotD-spermidine complex revealed that four acidic

residues (Glu36, Asp168, Glu171, and Asp257) and five aromatic residues (Trp34, Tyr37, Trp255, Tyr293, and Trp229) interact with the spermidine molecule. Although the structure of the PotD-putrescine complex remains unknown, mutational analyses suggest that the location of the putrescine molecule bound to PotD is equivalent to that of the diaminobutane moiety of the bound spermidine (21).

In the present study, we have determined the 1.8 Å X-ray structure of the PotD-spermidine complex. This detailed structure, refined at higher resolution, reveals the precise mechanism of spermidine binding to PotD, which was not clear in the 2.5 Å structure. To investigate the differences in the substrate specificity between PotD and PotF, we built a model of the PotF structure, using the PotD structure as a template.

5.3 Materials and methods

5.3.1 *Crystal Structure Determination and Refinement*

The PotD protein was crystallized in two different forms (monoclinic and tetragonal) in the presence of spermidine (Table 5.1). Procedures for crystallization and data collection were reported previously (22). The cocrystallizations of the PotD protein with spermidine were performed using the sitting drop method. The monoclinic form of PotD complexed with spermidine was obtained at 12 °C in a solution containing 15%(w/v) polyethylene glycol 10,000 and 10mM Bis-tris buffer (pH 7.0). The tetragonal form of the same complex was obtained from a crystallization drop containing the protein-spermidine mixture in 15% polyethylene glycol 4,000 and 10mM HEPES buffer (pH 7.0) at 20 °C. Intensity data were collected, using an automated oscillation camera system (DIP-320, MAC Science) with a

cylindrical imaging plate detector, and they were merged by the use of the program PROTEIN, version 3.1 (23).

Table 5.1

Crystal data and X-ray data processing statistics

	monoclinic form (Form I)[b]	tetragonal form (Form II)[b]
Space group	$P2_1$	$I4_1$
Cell constants (Å)		
a	145.3	130.3
b	69.1	130.3
c	72.5	38.7
β (°)	107.6°	
Resolution (Å)	∞ - 2.5	∞ - 1.8
Number of measured reflecions	141,071	246,531
Number of independent reflections	40,242	24,579
Completeness (%)	84.4	87.8
*R*merge[a](%)	9.4	9.1

[a]$R_{merge}=\Sigma|I-\langle I\rangle|/\Sigma|\langle I\rangle| \times 100$.
[b](22)

The crystal structure of the tetragonal form was solved using the molecular replacement technique, in which the structure of the monoclinic form refined at 2.5 Å resolution (10) was the search model. Rotation and translation functions were calculated using the X-PLOR program package

(24). A Patterson map for the tetragonal form was calculated using the observed intensities from 15.0 to 4.0 Å resolution. Another Patterson map for search was also calculated from data with the same resolution range, using the initial model in the space group $P1$ lattice, with unit cell dimensions of a=b=c=120 Å. The rotation search based on the PC-refinement procedure (24) provided one strong peak and the translation search also yielded a prominent peak. Rigid-body and simulated annealing refinements were then carried out with X-PLOR. After these refinement, the R-factor and R-free were reduced from 44.3% to 27.6% and from 43.8% to 36.4%, respectively, for data between 10.0 to 1.8 Å resolution. The (2|Fo| - |Fc|) electron density map showed obvious improvement for all of the protein atoms. The PotD and spermidine molecule could be fitted to the electron density without ambiguity. The refinement was subsequently performed using the programs PROTIN/PROLSQ (25) and CONEXN (26). Final R-factor was 19.8% for data from 6.0 to 1.8 Å resolution. Refinement statistics are summarized in Tables 5.2 and 5.3. Ramachandran plots for the main-chain torsion angles were analyzed with PROCHECK (27). All of the ψ and φ torsion angles for the non-glycine residues lie within the allowed regions.

5.3.2 *Modeling of the PotF Structure*

The model of the PotF structure was built according to standard homology modeling procedures. The 1.8 Å X-ray structure of PotD was used as a template for the model and alignment of the PotD and PotF sequences was achieved by the Needleman-Wunsch method (28), with slight manual modifications. The model was refined by energy minimization using the program PRESTO (29) to remove van der Waals clashes.

Table 5.2

Final refinement parameters of the PotD complex

Number of atoms	2,927
Number of solvent atoms	357
Number of spermidine atoms	10
Number of parameters	11,709
Resolution range (Å)	6.0-1.8
Number of used reflections	23,364
R-factor[a] (%)	19.8

[a]*R*-factor = Σ||Fo| - |Fc||/Σ|Fo| x 100.

5.4 Results and discussion

5.4.1 *Crystal Structure of the PotD-Spermidine Complex*

In this present work, the PotD-spermidine complex has been crystallized in a tetragonal form. The crystal contained one subunit in an asymmetric unit, whereas the monoclinic form, the structure of which was previously determined at 2.5 Å resolution, contained two dimers in an asymmetric unit (10). The crystal data of the monoclinic and tetragonal forms are summarized in Table 5.1. The average values of the root mean square deviations between the crystal structures of the monoclinic and tetragonal forms are 0.46 Å for all Cα atoms, 0.43 Å for the amino-terminal domain (N domain) Cα atoms, and 0.47 Å for the carboxyl-terminal domain (C domain) Cα atoms. Although the two crystals have different subunit interactions and molecular arrangements, these root mean square deviations are very small. This result suggests that the

Table 5.3

Weighting parameters in the final refinement of the PotD complex

Restraints	r.m.s. deviation[a]	Target σ[b]
Distance (Å)		
Bond	0.013	0.020
Angle	0.037	0.035
Planar 1-4	0.046	0.050
Planar groups (Å)	0.011	0.020
Chiral volumes (Å^3)	0.165	0.150
Nonbonded contacts (Å)		
Single torsion	0.186	0.300
Multiple torsion	0.215	0.300
Possible H-bond	0.243	0.300
Torsion angles (degree)		
Peptide planar (ω)	1.8	3.0
Staggered (±60 or 180°)	22.3	15.0
Orthogonal (±90°)	32.7	20.0
Isotropic B-factors (Å^2)		
Main chain bond	1.170	1.500
Main chain angle	1.866	2.000
Side chain bond	1.589	2.000
Side chain angle	2.243	2.500

[a] Root-mean-square deviation from ideality.

[b] The weight for each restraint was $1/\sigma^2$.

conformations between the N and C domains of PotD-spermidine complex are considerably rigid.

A crystal structure of the PotD-spermidine complex was determined at 1.8 Å resolution (Figure 5.1). The PotD molecule is divided into two domains, which are connected through two β strands and one short peptide segment. The two connecting strands form a hinge between the two domains, and this hinge lies at the bottom of the cleft. A similar folding pattern is exhibited by the two domains, consisting of a central β sheet and flanking α helices.

The PotD protein exhibits no significant sequence similarity with other periplasmic substrate-binding proteins, such as arabinose- (ABP), galactose/glucose- (GGBP), leucine- (LBP), leucine/isoleucine/valine- (LIVBP), maltodextrin- (MBP), sulfate- (SBP), and lysine/arginine/ornithine- (LAO) binding proteins (less than 20% sequence identity). However, the PotD protein and these periplasmic proteins share a similar α/β type fold, which consists of repeated β-α-β units. According to the differences in the detailed folding topology, these periplasmic binding proteins can be further classified into two groups, termed I and II (16). Group I contains ABP, GGBP, LBP, and LIVBP, and Group II includes MBP, SBP, and LAO. Group I has the β-sheet topology of the N domain represented as βn-βD-βC-βA-βB, while the topology of group II is βD-βn-βC-βA-βB. In this paper, the notation follows that of Spurlino *et al.* (16), and βn denotes the β strand that first occurs after the chain returns from the C domain. Therefore, the PotD structure belongs to group II. There is a single substrate binding site in these periplasmic binding proteins and it lies between the N and C domains. Several structures of these proteins are known with respect to both liganded and unliganded forms, which show that they undergo large hinge bending motions upon binding ligand. A similar process may occur in the PotD protein (10).

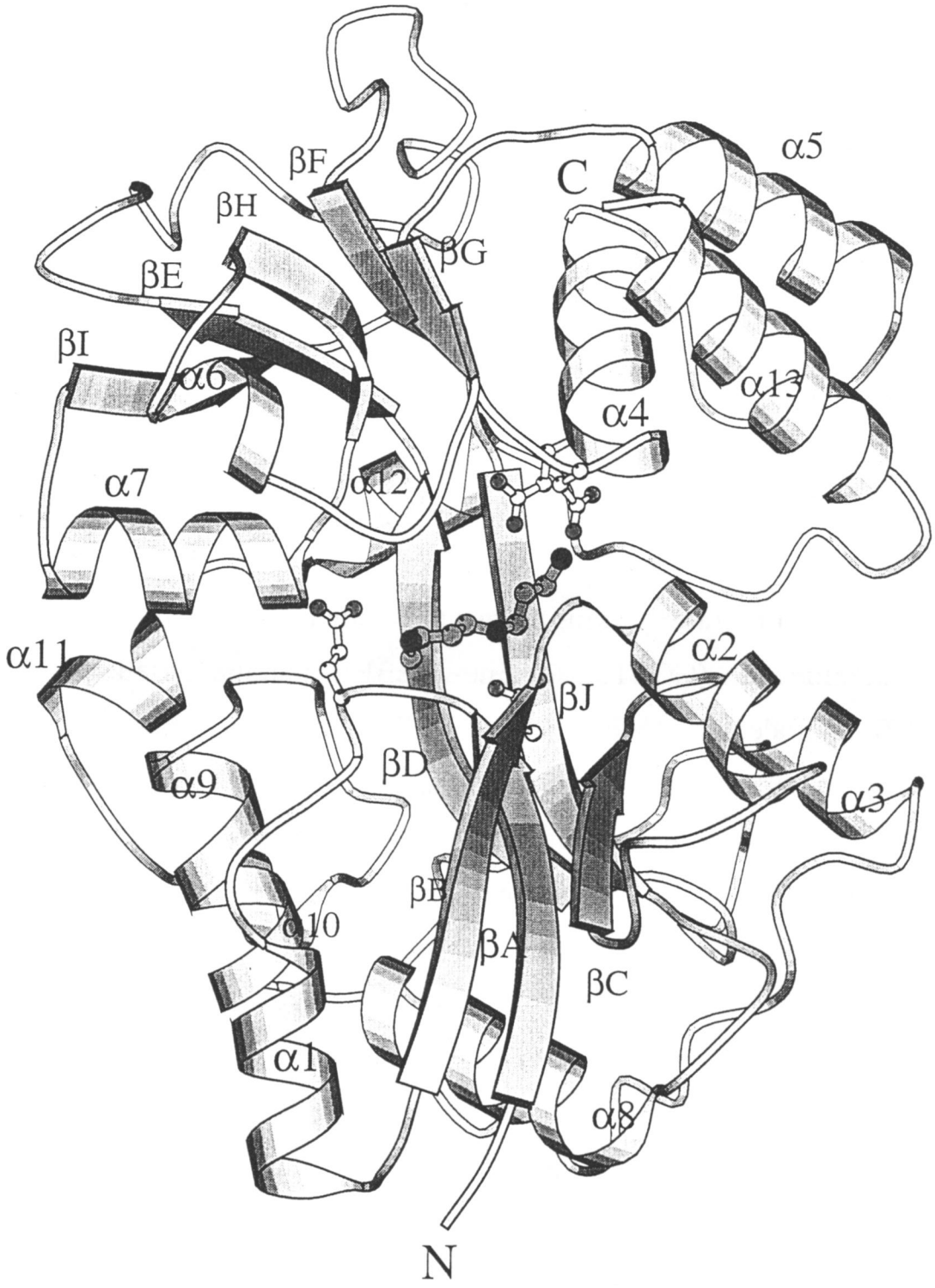

Figure 5.1 Overall structure and active site of the PotD protein.

This ribbon model of the PotD protein was drawn using the program MOLSCRIPT (32). The N domain lies at the bottom, and the C domain is at the top. The spermidine molecule is bound in the central cleft between the two domains. The four acidic residues in the active center are indicated by *ball and stick models*.

5.4.2 *Spermidine Binding*

The 1.8 Å X-ray structure clearly revealed a water molecule in the substrate-binding cleft of PotD. This solvent molecule, which was not observed in the 2.5 Å monoclinic crystal structure, formed a hydrogen bond with the terminal amino group of the aminobutyl moiety of the spermidine bound to PotD. Furthermore, it formed two hydrogen bonds to the hydroxyl group of Thr35 and the main chain carbonyl oxygen of Ser211. The hydrogen bonds and the salt bridge interactions between the spermidine, protein, and solvent molecules are summarized in Table 5.4.

Table 5.4

Hydrogen bonds and salt bridge interactions between spermidine, protein, and solvent

Protein/Solvent Residue	Atom	Spermidine Atom	Distance (Å)
Thr35	Oγ1	N3	3.36
Glu36	Oε2	N3	3.17
Tyr85	OH	N1	2.79
Asp168	Oδ1	N1	3.73
	Oδ2	N1	3.14
Glu171	Oε1	N1	2.78
Asp257	Oδ1	N2	3.53
	Oδ2	N2	2.93
Gln327	Oε1	N1	2.66
Wat	O	N3	2.70

Protein Residue	Atom	Solvent Residue	Atom	Distance (Å)
Thr35	Oγ1	Wat	O	3.01
Ser211	O		O	2.65

These findings are consistent with the results from mutational analyses (21), in which spermidine uptake activities were measured in intact cells expressing mutated PotD proteins. It was found that Glu171, Trp255, and Asp257 participated in the binding of spermidine more strongly than the others among the aforementioned amino acids. Furthermore, the mutant proteins in which Glu171, Trp255, and Asp257 was replaced, exhibited lower binding activities for spermidine among the various mutants.

The crystal structure of the free spermidine molecule has already been determined by two groups (30,31). We compared these structures with the 1.8 Å structure of spermidine bound to PotD (Figure 5.2). The torsion angles of spermidine trihydrochloride (30), spermidine phosphate trihydrate (31), and spermidine bound to PotD are listed in Table 5.5. Whereas the backbone conformation of the free spermidine molecule is almost flat, that of the form bound to PotD was bent. This suggests that the spermidine molecule is highly flexible and undergoes a large conformational change upon binding to the active site. Distortion of the spermidine conformation is likely to have been caused by the intermolecular contacts with the PotD protein.

5.4.3 *Substrate Specificity of Polyamine-Binding Proteins*

Another *E. coli* periplasmic polyamine binding protein, PotF, exhibits 35% sequence identity to PotD, implying that the overall architectures are well conserved between the two proteins. However, they have different substrate specificities. The PotD protein binds both spermidine and putrescine, with dissociation constants (*Kd*) of 3.2 μM and 100 μM, respectively (32). On the other hand, PotF binds only putrescine, with a *Kd* of 2.0 μM (7). The present structure, highly refined at 1.8 Å resolution, tempted us to examine how the two proteins could exhibit such different substrate specificities.

Table 5.5

Torsion angles of spermidine molecule

	Spermidine in protein	Spermidine trihydrochloride[a]	Spermidine phosphate trihydrate[b]	
			molecule I	molecule II
N(1) - C(1) - C(2) - C(3)	202.4	180.0	181.8	183.5
C(1) - C(2) - C(3) - N(2)	186.5	180.0	177.3	176.1
C(2) - C(3) - N(2) - C(4)	78.6	180.0	187.5	179.9
C(3) - N(2) - C(4) - C(5)	181.9	180.0	171.9	187.2
N(2) - C(4) - C(5) - C(6)	193.7	180.0	178.5	185.2
C(4) - C(5) - C(6) - C(7)	160.5	180.0	183.9	177.0
C(5) - C(6) - C(7) - N(3)	81.5	180.0	176.9	175.7

[a] (30), [b] (31)

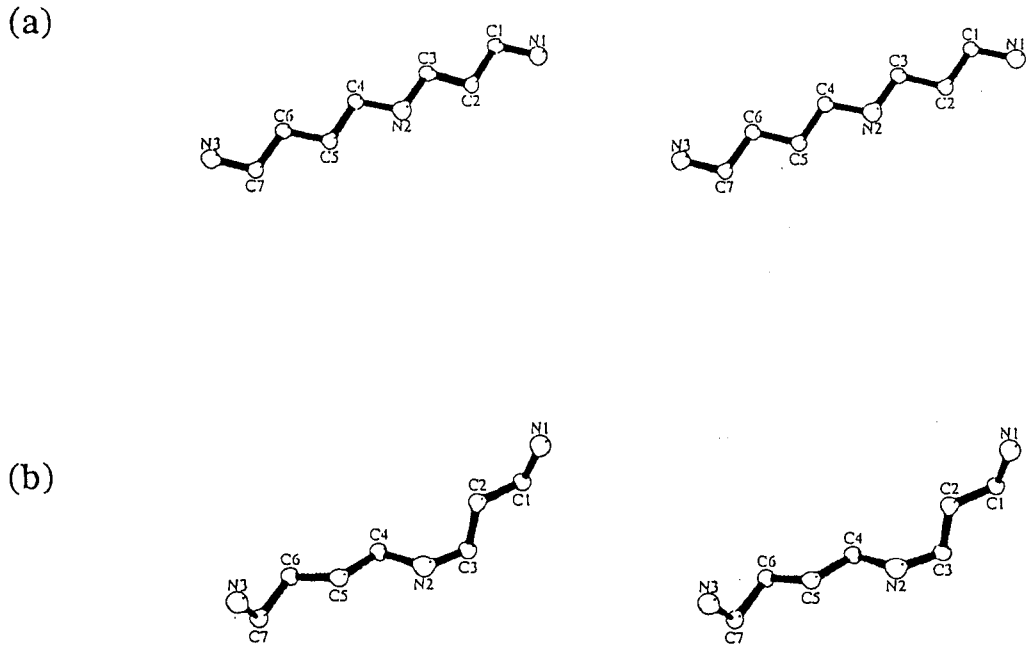

Figure 5.2 Stereo drawings of the atomic structures of spermidine molecules. (a) The spermidine trihydrochloride molecule (29). (b) The molecule in the tetragonal form of the PotD crystal.

(c)

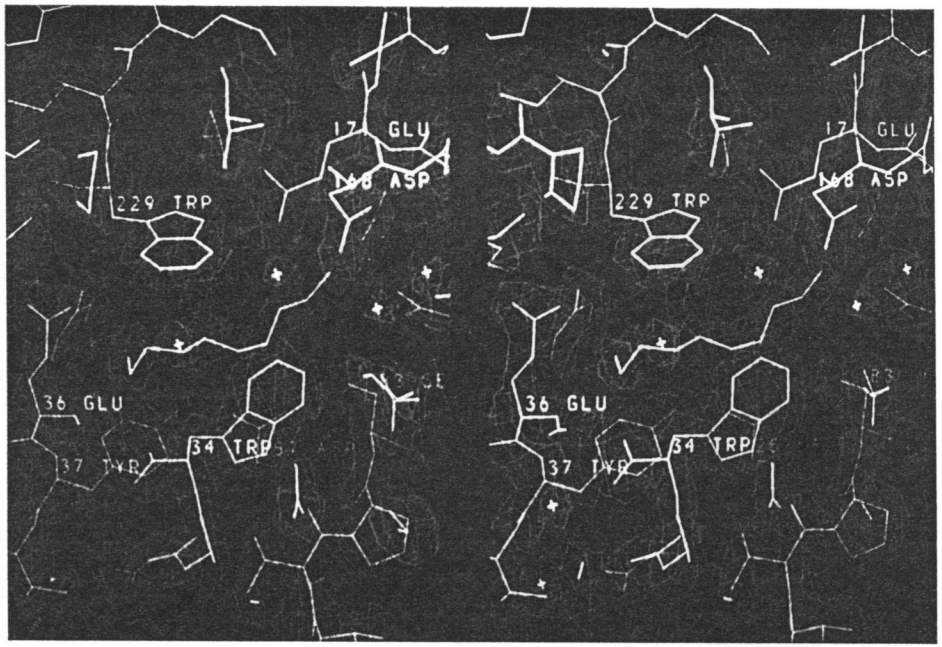

Figure 5.2 Stereo drawings of the atomic structures of spermidine molecules.

(c) The final $2|F_O| - |F_C|$ electron density around the bound spermidine molecule. The residues of the N-domain are *green*, the C-domain is *blue*, and the substrate is *red*.

The amino acid sequences of the PotD and PotF proteins were compared and aligned (Figure 5.3). Among the 14 residues of PotD involved in spermidine binding, eight (Trp34 with Trp37, Tyr37 with Tyr40, Ser83 with Ser85, Glu171 with Glu185, Ser211 with Ser226, Trp229 with Trp244, Asp257 with Asp278, Tyr293 with Tyr314) are invariant in PotF, and three are replaced by similar amino acids (Thr35 by Ser38, Glu36 by Asp39, and Trp255 by Phe276). Therefore, the different substrate specificity of PotF may be caused mainly by the substitutions at the remaining 3 residues (Tyr85 by Ser87, Asp168 by Ala182, and Gln327 by Lys349).

The side chain hydroxyl group of Tyr85 in PotD was hydrogen-bonded to the terminal amino group of the spermidine. Due to the conservation of the hydroxyl side chain, Ser87 of PotF may retain the hydrogen bond to the spermidine. The carboxyl group of Asp168 in PotD forms a hydrogen bond and a salt bridge with spermidine. Substitution of Asp168 by Ala182 may cause PotF to lose this strong electrostatic interaction with spermidine, and hence it decreases its ability to bind spermidine. In the PotD protein, the side chain of Gln327, which is hydrogen-bonded to the spermidine amino group, is replaced by Lys349 in the PotF protein. The positive charge of Lys349 could cause serious electrostatic repulsion against the positively charged amino group of spermidine, and would thereby greatly reduce the ability of the PotF protein to bind spermidine (Figure 5.4).

Putrescine is equivalent to the diaminobutane portion of spermidine, as it lacks the aminopropyl moiety. Mutational analyses indicated that, when bound to PotD, the putrescine molecule occupies the identical position to that of the diaminobutane portion of spermidine bound to PotD (21). It would be reasonable to assume that putrescine could be positioned in PotF in the same manner as found in PotD. The substitutions at the above three positions could therefore disturb spermidine binding by PotF, although they do not affect putrescine binding.

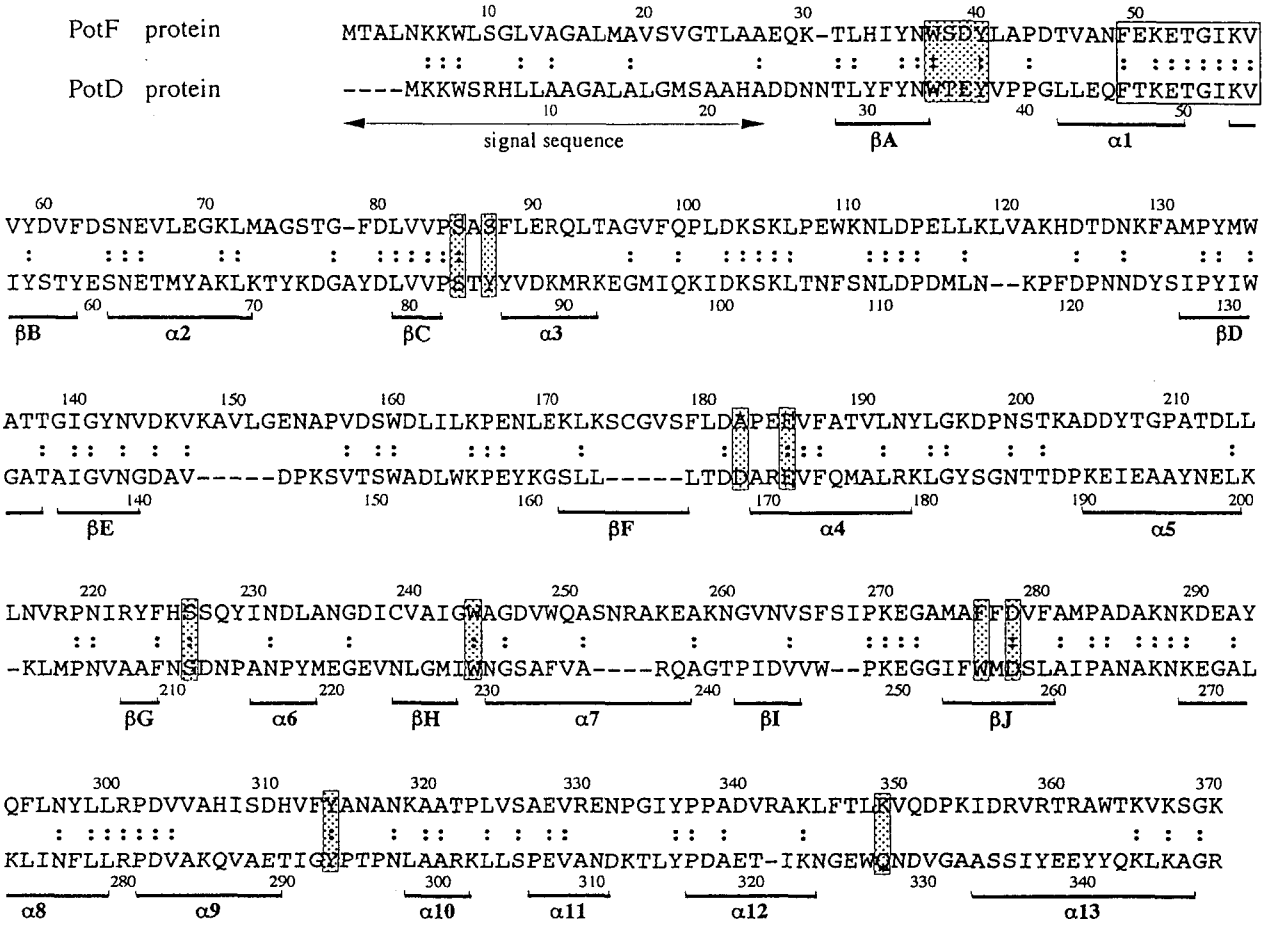

Figure 5.3 Sequence alignment between the PotD and PotF proteins.

Structurally equivalent residues are aligned. The gaps inserted for optimal alignment are indicated by '-'. Pairwise sequence comparison of PotF with PotD showed 34 % sequence identity. The active residues of PotD and the predicted active residues of PotF are indicated by the shaded boxes. A consensus motif region is indicated by a clear box. Fourteen residues of the PotD protein, Trp34, Thr35, Glu36, Tyr37, Ser83, Tyr85, Asp168, Glu171, Ser211, Trp229, Trp255, Asp257, Tyr293, and Gln327, which are involved in spermidine binding, are replaced by Trp37, Ser38, Asp39, Tyr40, Ser85, Ser87, Ala182, Glu185, Ser226, Trp244, Phe276, Asp278, Tyr314, and Lys349 in the PotF protein, respectively.

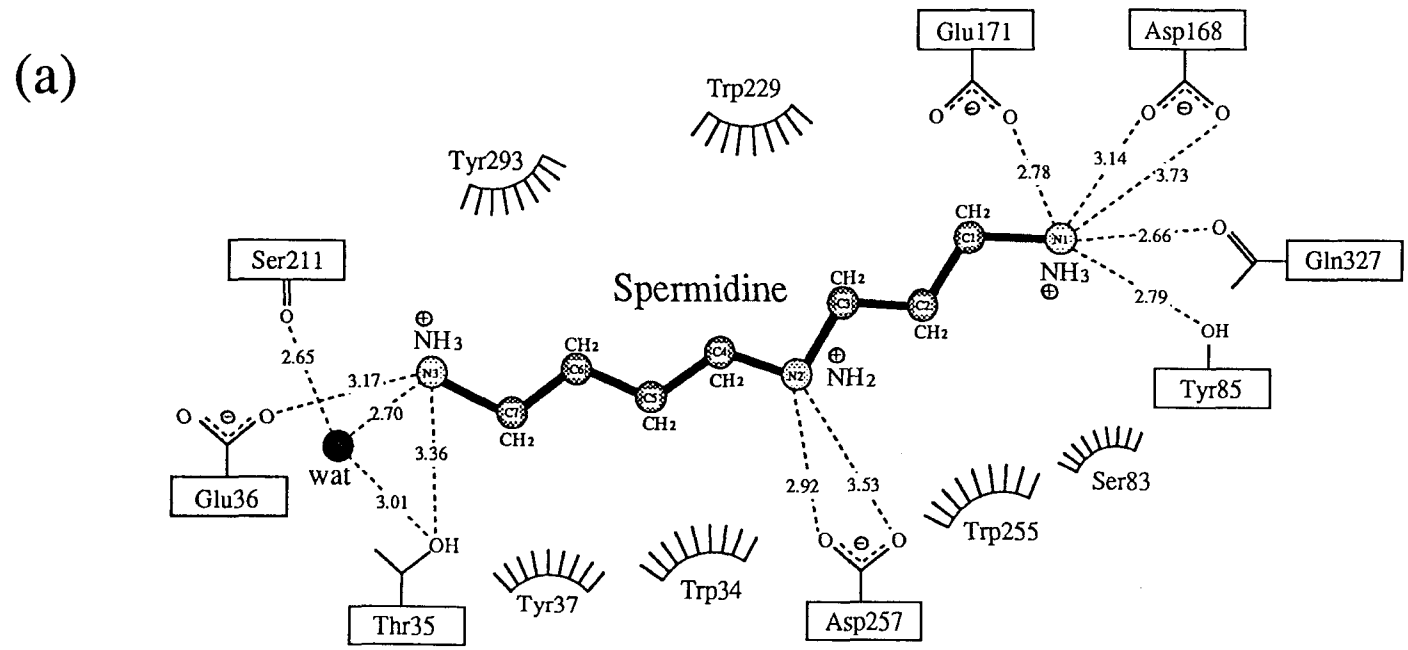

Figure 5.4 Interactions of spermidine with protein atoms.

Schematic diagram of electrostatic and van der Waals interactions with polyamine. (a) The active site of PotD. The methylene backbone of the spermidine makes van der Waals contacts with the aromatic side chains of five residues: Trp34, Tyr37, Trp229, Trp255, and Tyr293. All of the three charged amino groups of spermidine make electrostatic interactions with the PotD protein. The terminal amino group of the spermidine aminopropyl moiety forms hydrogen bonds and a salt bridge with the side chain carboxyl groups of Asp168 and Glu171, and is hydrogen-bonded to the side chains of Gln327 and Tyr85. The amino group in the middle of the spermidine molecule is recognized by the side chain of Asp257. The other terminal amino group forms hydrogen bonds with the carboxyl side chain of Glu36 and with the hydroxyl group of the side chain of Thr35.

(b)

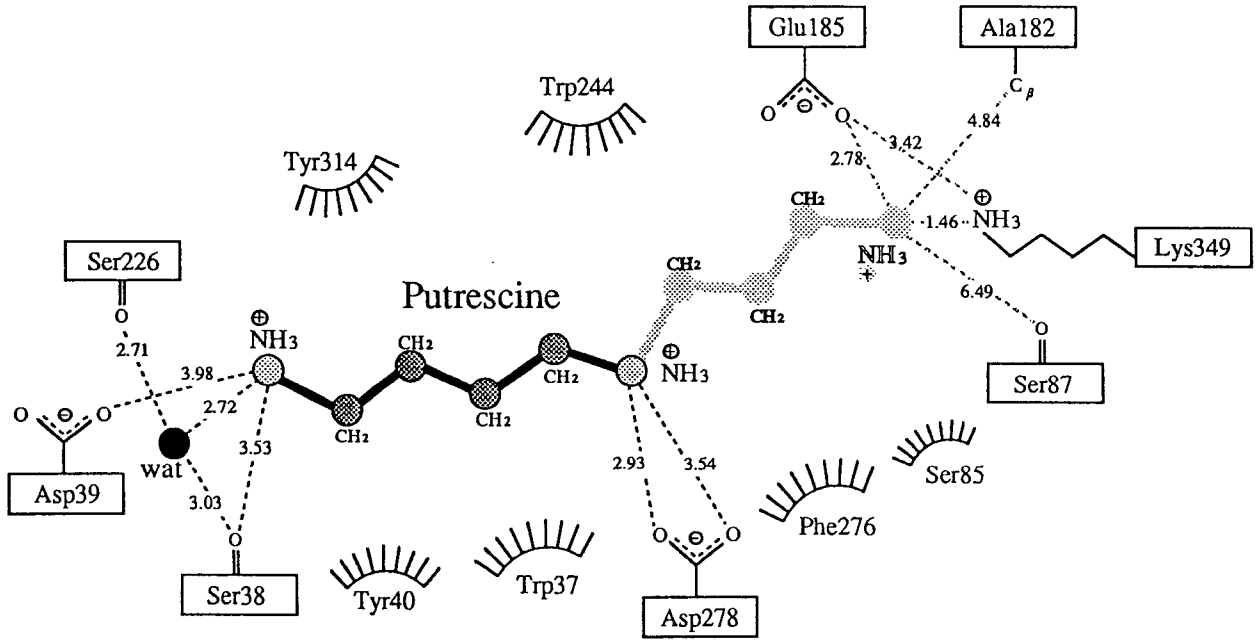

Figure 5.4 Interactions of spermidine with protein atoms.

(b) The predicted active site of PotF. It is mainly composed of five aromatic side chains, Trp37, Tyr40, Trp244, Phe276, and Tyr314.

To investigate these implications for binding, a three-dimensional structural model of PotF was constructed, using the 1.8 Å PotD-spermidine complex structure as a template. First, the PotF structure was modeled according to the sequence alignment in the PotD crystal structure. A spermidine molecule was then simply docked into the model, by assuming that it occupies the same position as in the PotD-spermidine complex.

The interaction of spermidine with PotF is shown schematically in Figure 5.4(b). In the model, Asp39 and Phe276 can interact with the spermidine molecule. The side chain hydroxyl group of Ser87 is 6.49 Å away from the terminal amino group of the aminopropyl portion of the spermidine. This distance is too large for Ser87 to hydrogen bond to the amino group. The distance between the two amino groups of Lys349 and spermidine is 1.46 Å, which generates serious steric hindrance.

In conclusion, the crystal structure of the *E. coli* PotD protein complexed with spermidine was determined at 1.8 Å resolution. The refined structure revealed a water molecule in the binding site of the PotD protein, and through this water molecule, the bound spermidine molecule forms two hydrogen bonds with Thr35 and Ser211. In addition to direct polar and van der Waals interactions, these indirect interactions should contribute to spermidine recognition. Furthermore, the PotD structure was found to be very similar to those of MBP, SBP, and LAO, which are members of the periplasmic binding protein superfamily. Structural comparison suggests that a large hinge bending motion, similar to those observed in these binding proteins, may occur in the PotD protein. The examination, based on the model building, led to the following putative mechanism of polyamine binding by PotF. Putrescine would interact with Trp37, Ser38, Asp39, Tyr40, Ser226, Trp244, Asp278, and Tyr314 of PotF. In contrast, PotF does not bind spermidine, particularly because the replacement of Gln327 of PotD by

Lys349 causes an unfavorable repulsion between the positive charges of its side chain and the terminal amino group of spermidine.

References

1. Tabor, C. W., and Tabor, H. (1984) *Annu. Rev. Biochem.* **53**, 749-790
2. Pegg, A. E. (1988) *Cancer Res.* **48**, 759-774
3. Kashiwagi, K., Hosokawa, N., Furuchi, T., Kobayashi, H., Sasakawa, C., Yoshikawa, M., and Igarashi, K. (1990) *J. Biol. Chem.* **265**, 20893-20897
4. Kashiwagi, K., Suzuki, T., Suzuki, F., Furuchi, T., Kobayashi, H., and Igarashi, K. (1991) *J. Biol. Chem.* **266**, 20922-20927
5. Kashiwagi, K., Miyamoto, S., Suzuki, F., Kobayashi, H., and Igarashi, K. (1992) *Proc. Natl. Acad. Sci. USA.* **89**, 4529-4533
6. Furuchi, T., Kashiwagi, K., Kobayashi, H., and Igarashi, K. (1991) *J. Biol. Chem.* **266**, 20928-20933
7. Pistocchi, R., Kashiwagi, K., Miyamoto, S., Nukui, E., Sadakata, Y., Kobayashi, H., and Igarashi, K. (1993) *J. Biol. Chem.* **268**, 146-152
8. Ames, G. F. L. (1986) *Annu. Rev. Biochem.* **55**, 397-426
9. Furlong, C. E. (1987). in *Escherichia coli and Salmonella typhimurium: Cellular and Molecular Biology* (Neidhardt, F. C., Ingraham, J. L., Low, K. B., Magasanik, B., Schaechter, M., and Umbarger, H. E., eds). pp. 768-796, American Society for Microbiology, Washington, D.C.
10. Sugiyama, S., Vassylyev, D. G., Matsushima, T., Kashiwagi, K., Igarashi, K., and Morikawa, K. (1996) *J. Biol. Chem.* **271**, 9519-9525
11. Quiocho, F. A., and Vyas, N. K. (1984) *Nature* **310**, 381-386
12. Vyas, N. K., Vyas, M. N., and Quiocho, F. A. (1988) *Science* **242**, 1290-1295
14. Sack, J. S., Saper, M. A., and Quiocho, F. A. (1989) *J. Mol. Biol.* **206**, 171-191

15. Sharff, A. J., Rodseth, L. E., Spurlino, J. C., and Quiocho, F. A. (1992) *Biochemistry* **31**, 10657-10663
16. Spurlino, J. C., Lu, G. Y., and Quiocho, F. A. (1991) *J. Biol. Chem.* **266**, 5202-5219
17. Pflugrath, J. W., and Quiocho, F. A. (1988) *J. Mol. Biol.* **200**, 163-180
18. Kang, C. H., Shin, W. C., Yamagata, Y., Gokcen, S., Ames, G. F. L., and Kim, S. H. (1991) *J. Biol. Chem.* **266**, 23893-23899
19. Oh, B. H., Pandit, J., Kang, C. H., Nikaido, K., Gokcen, S., Ames, G. F. L., and Kim, S. H. (1993) *J. Mol. Biol.* **268**, 11348-11355
20. Quiocho, F. A. (1991) *Curr. Opin. Struct. Biol.*, **1**, 922-933
21. Kashiwagi, K., Pistocchi, R., Shibuya, S., Sugiyama, S., Morikawa, K.,and Igarashi, K. (1996) *J. Biol. Chem.* **271**, 12205-12208
22. Sugiyama, S., Matsushima, M., Saisho, T., Kashiwagi, K., Igarashi, K., and Morikawa, K. (1996) *Acta Crystallogr.* **D52**, 416-418
23. Steigemann, W. (1974) Ph.D. thesis, Technishe Universität, München.
24. Brünger, A. T. (1992) *X-PLOR (Version 3.1) Manual.* Yale University, New Haven, CT.
25. Hendrickson, W. A. (1985) *Methods Enzymol.* **115**, 252-270
26. Pahler, A., and Hendrickson, W. A., (1990) *J. Appl. Crystallogr.* **23**, 218-221
27. Laskowski, R. A., MacArthur, M. W., Moss, D. S., and Thornton, J. M. (1992) *J. Appl. Crystallogr.* **26**, 283-291
28. Needleman, S. B. and Wunsch, C. D. (1970) *J. Mol. Biol.* **48**, 443-453
29. Morikami, K., Nakai, T., Kidera, A., Saito, M. & Nakamura, H. (1992) *Computers Chem.* **16**, 243-248
30. Giglio, E., Liquori, A. M., Puliti, R., and Ripamonti, A. (1966) *Acta Crystallogr.* **20**, 683-688
31. Huse, Y. and Iitaka, Y. (1969) *Acta Crystallogr.* **B25**, 498-509

32. Kashiwagi, K., Miyamoto, S., Nukui, E., Kobayashi, H., and Igarashi, K. (1993) *J. Biol. Chem.* **268**, 19358-19363

33. Kraulis, P. J. (1991) *J. Appl. Crystallogr.* **24**, 946-950

Chapter 6

Concluding Remarks

The polyamines are unique substrates for a binding protein. In the present study, the three-dimensional structure of PotD protein complexed with spermidine molecule has been solved at an atomic resolution by X-ray structure analysis. Therefore, it was the first time in which the detailed mechanism of its specific substrate recognition was elucidated.

In the Chapter 2, it is shown that two crystal forms of the PotD protein was obtained in the presence of spermidine molecule, and examined by X-ray analyse. The diffraction pattern from the monoclinic form crystal systematically indicates weak intensities for the *h* odd indexed reflections. The self-rotation function exhibited one significant peak. Moreover, the Patterson synthesis provided a strong non-origin peak. Thus, the non-crystallographic 2-fold axis was found to be approximately perpendicular to the crystallographic *b* axis. These results suggest that the protein molecules in the pair are related by the dyad axis, and that two pairs are packed with a local translation of approximate 1/2 of the unit cell length along the *a* axis.

In the Chapter 3, it is shown that the crystal structure of PotD in complex with spermidine, which was solved at 2.5 Å resolution, revealed the

feature of the overall fold structure and the polyamine binding activities in the PotD protein. The overall fold of PotD protein is similar to that of other periplasmic binding proteins. These findings are consistent with the results from the 3D-1D method by Matsuo *et al.* Furthermore, the highly conserved sequence motif was found in both PotD protein and MBP. It may be possible that the physiological role of the consensus sequence is to interact with the membrane components (PotB and/or PotC proteins). The PotD molecule forms a dimer in this crystal structure, although PotD exists as a monomeric form in the presence of the substrate in solution. The dimer is stabilized by a network of many hydrogen bonds and van der Waals interactions. These ionic interactions between the two subunits are so extensive that they are unlikely to have accidentally taken place during crystallization. Therefore, we assume that the switch from the dimeric form to the monomeric form of the PotD protein may have physiological significance in polyamine transport.

The PotD protein can bind putrescine as well as spermidine, although the affinity of putrescine is much lower than that of spermidine. The shorter putrescine molecule could possibly make ionic interactions with the acidic residues, and form van der Waals interactions with the aromatic residues. These interactions may stabilize the closed conformation. However, less interactions, compared with those with spermidine, would decrease the stability of the closed form.

In the Chapter 4, it is shown that spermidine binding sites on PotD protein, in the spermidine preferential uptake system were studied by measuring polyamine transport activities and polyamine binding activities of the mutated PotD proteins. It was found that 13 residues of PotD protein were involved in binding spermidine. These findings are consistent with the results from X-ray analysis. Putrescine is equivalent to the diaminobutane portion of spermidine, as it lacks the aminopropyl moiety. Mutational analyses indicated

that, when bound to PotD, the putrescine molecule occupies the identical position to that of the diaminobutane portion of spermidine bound to PotD.

In the Chapter 5, it is shown that the crystal structure of the PotD protein complexed with spermidine was solved at 1.8 Å resolution and revealed the detailed substrate binding mechanism. The structure provided the detailed conformation of the bound spermidine. Furthermore, a water molecule was clearly identified in the binding site, and involves in spermidine binding to PotD protein. The PotF protein, exhibits 35% sequence identity with the PotD protein, and it binds only putrescine. To understand these different substrate specificities, model building of the PotF protein was performed on the basis of the PotD crystal structure. The model structure suggests that the side chain of Lys349 in PotF inhibits spermidine binding because of the repulsive forces between the positive charges of the side chain and spermidine.

As shown in this thesis, the interactions between polyamine and acidic or aromatic residues play a key role in molecular recognition of polyamines. It is noteworthy that these interactions in the protein-polyamine complexes depend almost entirely on side chains of Glu, Asp, Trp, and Tyr. It is likely that this mechanism is similar to that of other proteins, which recognize the polyamine molecules.

The highly conserved motif which is observed in PotD protein, MBP, and IBP, is assumed to have the important role in these transport systems. However, its function is not elucidated yet. The mutation analysis on this region is necessary to understand its function, which will be elucidated by further studies.

Nearly all large proteins are built with domains. Domain motions are important for a variety of protein functions, including catalysis, regulation of activity, transport of metabolites, formation of protein assemblies, and cellular locomotion. These domains often close a binding site which is near the

interface. Generally, the presence of bound substrates stabilizes a closed conformation, and their absence favors an open conformation. Consequently, such domain motions illustrate an induced fit in substrate recognition by these proteins. In fact, among the periplasmic binding proteins, some proteins have been solved in both the states of open and closed conformations by X-ray analyses. The same may be said of PotD protein.

Finally, I would like to two approaches for the development of novel anti-cancer drugs using polyamine uptake inhibitors. The first is a way to design antagonists against the polyamine binding proteins based on three-dimensional structure of the PotD-spermidine complex. The compounds, which may make the electrostatic and the van der Waals interactions with the acidic residues and aromatic residues on the active site of PotD, are possible to be looked up from the Cambridge structural data base. They may become lead compounds for polyamine antagonists. Furthermore, three-dimensional structures of PotD complexed with the lead compounds will be studied by X-ray analysis. Therefore, it is likely that the affinity between PotD protein and antagonists increases further by regulating the size of hydrophobic functional groups on antagonists and introducing new functional groups into antagonists for hydrogen bonds with PotD protein, based on their three-dimensional structures. The other is a way to design a polyamine derivative which does not have the physiological activity, although it is transported into cellular by polyamine binding proteins. The cellular polyamine contents may decrease by being accumulated a large amount of polyamine derivatives in cell. The second is a way to design polyamine uptake inhibitors based on a structure of the conserved sequence motif region, which lies on the PotD protein surface, is a strong candidate to interact with the membrane components, PotB and/or PotC. It may be possible that a peptide or non-peptide compound, which mimics the three-dimensional structure of the conserved sequence motif

region, controls the polyamine uptake system by inhibiting the interaction between the membrane components and the PotD protein. Thus, if the cellular polyamine contents decrease by these ways, it is likely to inhibit the cell proliferation. These ways will be possible to apply for animal cell.

I hope that the present findings described in this thesis can be helpful for further studies.

The atomic coordinates and the structure factors have been deposited in the Protein Data Bank (PDB), Brookhaven National Laboratory, Upton, NY. These PDB ID codes of the monomer form are 1POT and R1POTSF, and these of the dimer form are 1POY and R1POYSF, respectively.

List of Publications

The contents of this thesis are compose of the following papers.

1. Sugiyama, S., Matsushima, M., Saisho, T., Kashiwagi, K., Igarashi, K., and Morikawa, K. (1996) Crystallization and Preliminary X-ray Analysis of the Primary Receptor (PotD) of the Polyamine Transport System in *Escherichia coli*. *Acta Crystallogr.* **D52**, 416-418

2. Sugiyama, S., Vassylyev, D. G., Matsushima, T., Kashiwagi, K., Igarashi, K., and Morikawa, K. (1996) Crystal Structure of PotD, the Primary Receptor of the Polyamine Transport System in *Escherichia coli*. *J. Biol. Chem.* **271**, 9519-9525

3. Kashiwagi, K., Pistocchi, R., Shibuya, S., Sugiyama, S., Morikawa, K., and Igarashi, K. (1996) Spermidine-preferential uptake system in *Escherichia coli*: Identification of amino acids involved in polyamine binding in PotD protein. *J. Biol. Chem.* **271**, 12205-12208

4. Sugiyama, S., Matsuo, Y., Maenaka, K., Dmitry, G. V., Matsushima, M., Kashiwagi, K., Igarashi, K., Morikawa, K. (1996) The 1.8 Å X-ray structure of *Escherichia coli* PotD protein complexed with spermidine and mechanism of polyamine binding. *Protein Science* **5**, 1984-1990

5. Sugiyama, S., Igarashi, K., Morikawa, K. (1996) The structure and function of the polyamine binding protein. *Seikagaku* **69**, 371-377

Acknowledgments

This work on structure analyses of polyamine-binding protein has been carried out in Protein Engineering Research Institute (6-2-3 Furuedai, Suita, Osaka 565, Japan) from 1993 to 1995.

The author would like to express his sincere gratitude to Dr. Kosuke Morikawa in Biomolecular Engineering Research Institute, and Dr. Masaaki Matsushima in Rational Drug Design Laboratories for their guidance, discussions, and intimate encouragements throughout this investigation.

The author is deeply grateful to Professor Kazuei Igarashi and Dr. Keiko Kashiwagi for providing his with purified protein and their discussions throughout this investigation.

The author wishes to make a grateful acknowledgment to Dr. Katsuo Katayanagi in Mitsubishi Kasei Co., Ltd. and Dr. Osamu Hiraoka for his incessant and his stimulating discussions throughout this investigation.

The author is deeply thankful to Drs. Ken Nishikawa in National Institute of Genetics, Yo Matsuo and Fumio Inoue in Fujitsu Laboratories Ltd., S. Hayashi, Tsuyoshi Ito, and all members in the fifth department in Protein Engineering Research Institute for computing support and their technical advice.

Grateful acknowledgment are given to Drs. Masato Shimizu, Satoshi Nureki, Dmitry G.Vassylyev, Tatsuki Kashiwagi, Haiwei Song, Katsumi Maenaka, Takahiko Sakuma, and all members in the first department in Protein Engineering Research Institute for the technical support and their helpful discussions.

The author deeply indebted to Drs. Mamoru Kohata, Reiji Matsuda, Hajime Yoshida, Mayumi Yoshida, and Yuuji Oda in Kyowa Hakko Kogyo

Co., Ltd., Dr. Junichi Sugai, and Dr. Yukihisa Matsuda in Biomolecular Engineering Research Institute for giving me his invariable advice.

The author is also grateful to Professor Yasushi Kai, Dr. Tsuyoshi Inoue, and all the members in Kai's laboratory of Osaka University for their collaboration in this work and kind assistance.

The author is deeply indebted to Professor Noritake Yasuoka, Drs. Yukio Morimoto and Shintaro Misaki in Himeji Institute of Technology, Dr Yoshiki Higuchi in Kyoto University, and in Tokushima University.

The author also thanks to Drs. Tomoyuki Matsumoto and Kazuo Kadogami in MAC science Co., Ltd. for their technical advice in DIP320 system of X-ray detector.

Finally, the author wishes to express his deep thanks to his parents and Matsuyama family for their perpetual assistance and encouragement.

Shigeru Sugiyama